

AD-A020 535

LEAD INITIATION BY M55 DETONATOR ACROSS AIR GAP

W. G. Schmacker, et al

Picatinny Arsenal
Dover, New Jersey

December 1975

DISTRIBUTED BY:

NTIS

National Technical Information Service
U. S. DEPARTMENT OF COMMERCE

**Best
Available
Copy**

050103

DA020535



COPY NO. 19

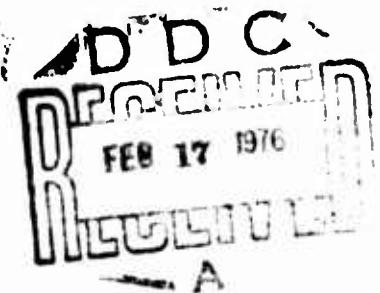
TECHNICAL REPORT 4779

**LEAD INITIATION BY M55 DETONATOR
ACROSS AIR GAP**

**W. G. SCHMACKER
W. E. VORECK**

DECEMBER 1975

APPROVED FOR PUBLIC RELEASE; DISTRIBUTION UNLIMITED.



**PICATINNY ARSENAL
DOVER, NEW JERSEY**

Reproduced by
**NATIONAL TECHNICAL
INFORMATION SERVICE**
U S Department of Commerce
Springfield VA 22151

The findings in this report are not to be construed as an official Department of the Army Position.

DISPOSITION

Destroy this report when no longer needed. Do not return to the originator.

ACCESSION for	
NTS	WHILE SERVING <input checked="" type="checkbox"/>
OC	DATE OF ISSUE <input type="checkbox"/>
UNANNOUNCED	<input type="checkbox"/>
JUSTIFICATION	
BY	
DISTRIBUTION	
AVAIL. END OF SERVICE	
Dist.	
A	

The citation in this report of the names of commercial firms or commercially available products or services does not constitute official endorsement or approval of such commercial firms, products, or services by the U. S. Government.

FOREWORD

This program was partly sponsored by the Explosives Division, Feltman Research Laboratory, and partly by the Ammunition Development & Engineering Directorate, Project GG28139.

Dr. Schmacker, from the Federal Forces Test Center 91, Meppen, Federal Republic of Germany, was a participant in the U. S. Exchange Program for Scientists and Engineers, Group No. 20.

ACKNOWLEDGMENT

The authors wish to thank Mr. J. Hershkowitz for many helpful comments he made on the tests conducted during this effort, and the assistance rendered in the preparation of this manuscript. They also wish to express their gratitude to Dr. R. Gentner for the TIGER computer program calculations, Mr. N. Palmer for the sieve analysis of RDX, Mr. E. Dalrymple for loading samples, and Mrs. L. Millington for drawing the figures.

TABLE OF CONTENTS

	Page No.
Summary	1
Introduction	2
Overall Transfer Time	2
Test Apparatus and Assemblies	2
Trigger Switches for t_{OT} Measurement	3
Detonators and Lead Cups	4
Calculating Excess Transit Time	7
Appropriate Hole Diameter in Standoff Spacer	7
Results: Overall Transit Time	8
Effect of Hole Diameter in Standoff Spacer	8
Effect of RDX Particle Size on Lead Initiation	8
Influence of Flyer Plates on Lead Initiation	10
Initiation of Lead Cups No. 2, 3, and 4	11
Influence on Detonation of the Covering of the Lead	13
Use of the Detonation Electric Effect for Lead Initiation Studies	13
Circuit Diagram for t_{OT} and DEE	14
DEE Profile	14
Results: Use of the DEE for Lead Initiation Studies	15
Influence of Foil Thickness on Calculated Excess Transit Times	15
Shock Wave and Fragment Velocities from DEE Measurements	15
Influence of Detonator on Lead Initiation	16
Replacement of M55 Aluminum Foil Closure with Teflon/Paper	17
Conclusions	17

References	19
Appendix Effect of Varying M55 Closure Disc Thickness on Acceptor (Lead) Transit Time	75
Distribution List	79

Tables

1	Spacings (L) between detonator and lead cup	21
2	Lead cup, dimensions and types	22
3	Lead cup explosives, components	23
4	Density vs loading pressure for lead cup explosives	24
5	Effect of reduced donor source areas on overall transfer times	25
6	Overall transit times for RDX classes C, A, and E	26
7	Experimental data on effect of RDX particle size and density in lead on initiation	27
8	TIGER code calculated ideal detonation time	28
9	Calculated excess transit times	29
10	Overall transit times for varied thicknesses of flyer discs	30
11	Influence of flyer plates on calculated excess transit times in lead explosives	31
12	Overall transit times of lead cups No. 2, 3, and 4, hole .055" dia	32
13	Overall transit times of M219 lead cups No. 2 and 4	33
14	Travel times of shock and fragments for M55 detonator Lot LS-DZ-3347 and ideal detonation times of used cups No. 2 and 4	34

15	Calculated excess transit times (in nanosec) for lead cups No. 2 and 4 in test assembly shown in 2.1 of Figure 2	35
16	Overall transit time for varied foil thickness on lead cup No. 3	36
17	Overall transit time for varied foil thicknesses on lead cup No. 4	37
18	Nylon washer lead No. 5, time measurements from DEE-profile	38
19	Lead No. 5, inert acceptor transit time measurements from DEE-profile	39
20	Mean times and velocities for shock and fragments of M55 detonator, lot IOP-1-74, across a gap of 0.068"	40
21	Excess transit times for nylon washer lead No. 5 with coverings of 2, 5, and 10 mil Al foil	41
22	Lead cup No. 4, time measurements from DEE-profile	42
23	Lead cup No. 4, velocities of shock and fragments	43
24	Influence of gap on shock and fragment velocities of M55 detonators	44
25	Calculated excess transit times for lead cup No. 4 with a 0.091" gap	45

Figures

1	Test apparatus for overall transit time measurements	47
2	Test assemblies for t_{OT} measurements	48
3	Start trigger switch at base of detonator	49

4	Stop trigger switches	50
5	Pin switch circuit	51
6	Illustration of detonation effect explosives configuration	52
7	Lead cup dimensions	53
8.1	Particle size distribution of RDX, Class C	54
8.2	Particle size distribution of RDX, Class A	55
8.3	Particle size distribution of RDX, Class E	56
8.4	Particle size distribution of RDX, Class G	57
8.3.1	RDX Class E, fractions 22 μ and 74 μ	58
9	Lead cup No. 4 - photograph of a cut through the aluminum case parallel to the center axis (height = 0.1104 in.)	59
10	Influence of RDX particle size and loading pressure on the compacted density	60
11	Detonation velocity vs density of RDX	61
12	Space-time plot of shock initiation (Ref 8)	62
13	Witness disc penetration in relation to the hole diameter in the standoff spacer (Configuration 2.1 of Figure 2 with 0.0864" spacing)	63
14	Witness disc penetration (by lead cup No. 1) in relation to RDX particle size (Class C, A, E) and loading pressure	64
15	Lead cup No. 3: Photograph of the coined bottom (see Figure 4), scale ca. 14:1	65

16	Lead cup No. 4: Photograph of the bottom area	66
17	Detonation transfer and detonation electric assembly	67
18	Test assemblies for DEE and overall transit time measurements	68
19	Circuit diagram for transit time (t_{UT}) and DEE	69
20	Explanation of the detonation electric effect records	70
21	Detonation electric effect records	71
22	Overall transit time vs foil thickness	72
23	Effect of closure disc thickness on acceptor transit time	73

SUMMARY

Studies were made of the detonation transfer between M55 detonators (donor) to the RDX loaded explosive lead¹ cups (acceptor) with the spacings normally used in fuzes. Methods were developed for measuring explosive acceptor detonation times and electric effect (DEE), and these were then used to quantitatively determine the efficiency of the initiation. The DEE also provided information on shock and fragment velocities produced by the detonator. Excess transit time calculations for the acceptors showed that initiation can be produced by shock alone, or in combination with fragments. Effects of variations in detonator closure discs, lead cup bottom thickness, as well as explosive type, particle size, and density were investigated.

¹"Lead", as used in this report, is pronounced to rhyme with "weed". It refers to a small explosive charge in a cup, used to transfer a detonation from a detonator to a larger explosive charge.

INTRODUCTION

The detonation transfer from a detonator to an acceptor (explosive-loaded lead cup) must be reliable to prevent duds and low order detonations in ammunition. The recent improvement of electronic time interval meters and oscilloscopes to one nanosecond accuracy has made possible investigation of short time events such as occur over the short distances in explosive trains. Improved methods were developed for measuring the factors governing the transfer of the detonation from detonator to acceptor (lead) by comparing excess transit times calculated from measurements of overall transfer times in the train, and by measuring the DEE from the explosive in the acceptor. Because of the limited number of tests, results could only be compared using 90% confidence limit (C/L) for the means (\bar{x}). The equation used (Ref 1) was

$$C/L = \bar{x} \pm \frac{1.86 s}{\sqrt{N}}$$

OVERALL TRANSFER TIME

Test Apparatus and Assemblies

The investigation started by measuring the overall transfer time (t_{OT}) by means of the apparatus shown in Figure 1, which consists of the test assembly with detonator and acceptor, an explosive-loaded lead cup, the support base, and the stab firing pin device for the detonator to assure reliable initiation. The standard M55 firing needle described by Voreck et al (Ref 2) was accelerated by a spring to an energy much higher than the 3/4 in.-oz required for 100% initiation (Ref 3). For electrical shielding and fragment containment, the test apparatus was placed within an aluminum enclosure of inside dimensions 4" diameter, 3" high. Holes in the sides were provided for electrical cables.

The parts in the test assemblies used are shown in Figure 2. In configurations 2.1 and 2.3 the explosive lead orientations correspond to that within a fuze, while 2.2 has the lead upside-down to provide a means to control the foil thickness over the explosive. Configuration 2.3 differs from 2.1 in that the gap is longer in 2.3 and variable with the additional nylon standoff washer used (Item 11). The spacings (L) between the bottom of the detonator and the covering of or over the lead cup were

varied between 0.086" and 0.126". Table 1 lists the data on the spacings (L) for the test assemblies shown in Figure 2; the various lead cups used are listed in Table 1. The spacings used depended upon the dimensions of the parts available, and were somewhat longer than those used in fuze trains in order to emphasize differences in initiation. All parts were clamped together to prevent variations in spacings.

Below the Al foil (Item No. 12) in the 2.2 configuration of Figure 2 there was an air gap of about 3.5 mils between the foil and the explosive. To determine if this was important, the Al foil diameter was reduced to 0.132" and placed in contact with the lead explosive. The gap spacing increased when this was done from 0.0981" to 0.1016" (Table 1, from L_4 to L_4).

In order to increase the sensitivity of the test and to simulate the effect of the detonators being partially out of line, the hole in the standoff spacer of steel (Item 6 in Fig 2) at the bottom of the detonator was made smaller to reduce the detonator output. The hole variation of 0.110", 0.078", 0.055", and 0.038" in diameter provided relative hole areas of 1, 1/2, 1/4, and 1/8.

Between standoff spacer and lead cup, the nylon confinement (Fig 2, Item 9) or the nylon distance washer (Fig 2, Item 11) provided an impedance mismatch and geometry to attenuate the shock wave through the housing material. Thus initiation of the explosive in the lead cup was achieved only by the shock and fragments which traveled across the air gap of spacing (L). This was shown by obtaining only no-fires when the hole was decreased to 0.038" diameter, or eliminated.

Trigger Switches for t_{OT} Measurement

The trigger switches for time interval measurements were located at the bottom edge of the detonator and at the base of the lead cup as shown in Figures 2, 3, and 4. The start trigger switches used (see Fig 3) consisted of two coplanar one-mil stainless steel foils spaced about a 1/32" apart and sandwiched between two insulating tapes (2.5 mil thick cellulose acetate). The shock wave from the detonation ionized the air in the gap to permit a flow of electricity. The start trigger switch was placed at the edge of the detonator bottom and so located as not to obstruct the fragment travel from the closure disc. Each of two stop switches used for t_{OT} measurements covered the whole area of the lead cup base (see Fig 4).

The gap between the copper strips in Switch No. 1 was replaced by the thickness of the tape (2.5 mil) in Switch No. 2. The closure of Switch No. 2 by the output of the lead cup, presumed not to be metal-to-metal contact, gave an improved signal. Start and stop switches were connected through a dual pin switch circuit, shown in Figure 5, which provided opposite polarity pulses from the two trigger switches to a 796 Eldorado time-interval meter, accurate to one nanosecond.

Detonators and Lead Cups

Dimensions and Explosives

All tests were run with an M55 detonator as the donor. The M55 design is shown in the upper part of Figure 6. It has an aluminum closure disc 3 mils thick at the bottom, which contributes to detonation transfer by fragmentation. The M55 detonators used were from

Lot LS-DZ-3347 made at Lone Star AAP, Texarkana, Texas

Lot IOP-1-74 made at Iowa Ordnance Plant, Burlington, Iowa

To determine the contribution of fragments from the closure disc, a special lot of M55 detonators, closed with a Teflon/paper laminate instead of an aluminum closure disc, was used:

Lot KN-E-26 made at Sunflower AAP, Lawrence, Kansas

The lead cups (LC) used as acceptors were given type numbers as follows:

- No. 1 Experimental Lead Cup, loaded by Picatinny Arsenal, drawing No. SK-BP-123, 3/8/73
- No. 2 M219 Lead Cup, Drawing No. 8833562, loaded by Picatinny Arsenal
- No. 3 M42 Grenade Lead, Lot LS-91-12
- No. 4 M219 Lead Cup, Lot LS-95-10
- No. 5 Explosive passed into nylon washer (described later in this report)

The dimensions of these lead cups as illustrated in Figure 7, are listed in Table 2. The values are averages of 3 to 5 measurements. Lead explosive compositions are shown in Table 3.

Particle Distribution of RDX for Lead Cup No. 1

For the experimental lead cups (No. 1) three lots of RDX were used as follows:

Type B, Class C, Lot HOL-8-45

Type B, Class A, Lot HOL-21-18

Type B, Class E, Lot HOL-42-57

The cumulative particle size distributions of RDX class C and A are shown in Figures 8.1 and 8.2. Plotted values are from sieve analyses with U. S. Standard sieves. The RDX samples, about 20 g each, were washed with 50 ml antistatic water (1 drop DOW-ECR-34 per liter distilled water) before screening and then dried at 60°C for 1 hour under vacuum. The measured values are compared in these figures with specification requirements (Ref 4) and values of Stott et al (Ref 5) on a different lot measured with the Mine Safety Appliance (MSA) Analyser, which is valid only up to 200 microns particle size.

The results shown in Figures 8.1 and 8.2 for Lots HOL-8-45 and 21-18 are approximated by straight lines, and therefore their particles follow normal distributions. The mean particle size at 50% was taken to characterize these RDX lots. The sieve analysis of HOL 21-18 did not meet specification requirements; this could be due to loss of fine RDX in this test method.

The particle size distribution of RDX class E (Lot HOL-42-57) was determined by a Cahn sedimentation balance. The method applied by Hutchinson (Ref 6) using water as sedimentation liquid gave good reproducibility. The 100 mg RDX samples were wetted, before analysis, with water of reduced surface tension (2 drops di-octyl sodium sulfosuccinate per 1 ml distilled water). The measured values were plotted on probability paper (Fig 8.3) and compared with data from Stott et al (Ref 5). Up to 30-micron particle size, the data of Lot HOL-42-57 is almost identical with that on the same lot by Stott et al. From the two straight line segments in

Figure 8.3, it is apparent that the RDX was a bimodal blend of two size fractions. The data of the 72.8% fine fraction and the 27.2% coarse fraction were plotted in Figure 8.3.1, confirming the bimodality. They show average particle sizes of 22 microns for the fine fraction and 74 microns for the coarse one. The RDX class E particle size was, therefore, characterized as 22.74.

Densities of Lead Explosives

The densities of lead explosives were calculated using the explosive weights measured on ten lead cups, the explosive volumes calculated with the average dimensions listed in Table 2, and the geometrical shape illustrated in Figure 7. The mean thickness (X) (see Fig 7) of the explosive covering was calculated by the equation below involving the thickness A of the coined area, the thickness B of the rim, the diameter of the coined area (D_c) and the interior of the cup (D_i)

$$X = B - (B-A) (D_c/D_i)^2.$$

The real shape of the interior of the lead cup differs from the geometrical shape as shown for lead cup 4 in Figure 9. The real volume appears a little larger than the volume calculated with the geometrical dimensions of Figure 7. The calculated densities listed in Table 4 contain a small systematic error, but are correct as relative values.

The densities of lead cup 1 explosives were plotted vs the loading pressure as shown in Figure 10. The fine particle size of RDX class E needs higher loading pressures to get the same densities as A and C. With larger particle sizes of RDX classes C and A, densities are higher for the same loading pressure, and the compressibility is less than for class E.

TIGER computer program calculations (Ref 7) provided a relation between detonation velocities and explosive densities for ideal detonation conditions. The computed curves for explosives used in lead cups 1 and 4 are shown in Figure 11. Actual velocities are somewhat lower due to the small diameter of the charges for pure RDX class C.

Calculating Excess Transit Time

The measured overall transit time t_{OT} (interval between trigger pulses) was used to obtain the calculated excess transit time (t_{cal}). Figure 12, after Ramsay and Popolato (Ref 8), illustrates the loci of propagation velocities in the lead cup under ideal and real conditions in the period before and after initiation. The transit time of the detonation through the lead explosive (t_{trans} in Fig 12) starts when the stimulus arrives. This point in time was obtained by subtracting from the overall transit time either the time of flight of fragments across the gap L (see Fig 2) or the time required for a shock wave to cross the gap (t_{frag} or t_{shock} in Fig 12). The times t_{frag} and t_{shock} were determined from the profiles to be described later in this report. The transit time (t_{trans}) ends when the detonation reaches the base of the lead cup.

The ideal transit time (t_{id}) with high order detonation and no delay in initiation can be calculated from the length h (Fig 6) of the explosive column in the lead and the ideal detonation velocity for the composition and density of the explosive (Fig 11). The values used were obtained from TIGER computer program calculations (Ref 7).

The excess transit time is the time required by the detonation to propagate across the lead in excess of that resulting from its immediate onset. The calculated excess transit time (t_{cal} in Fig 12) is the difference $t_{trans} - t_{id}$. As shown in Figure 12, the true excess transit time (t_{ext}) can be even larger than the calculated one by an error term t_e which is associated with the case where steady state detonation is not achieved within the length of explosive in the lead cup.

Appropriate Hole Diameter in Standoff Spacer

To simulate the effect of deficient output detonators or off center alignment of detonator to explosive lead, and to emphasize the differences between various lead cups, it was desirable to attenuate the output of the typical M55 detonators available for use in this program. Since increasing the spacing between the detonator and the explosive acceptor attenuates the shock wave but not the fragments, it was decided to retain normal spacing and attenuate both outputs by reducing the area of the detonator exposed to the lead.

Fragments from an M55 originate from both the closure disc and the crimped-over metal holding it in place. Fragmentation of the detonator was restricted to fragments from the 3-mil closure disc when the hole in the standoff spacer was smaller than the 0.100" diameter of the opening in the crimp around the rim at the base of the detonator (Fig 6).

RESULTS: OVERALL TRANSIT TIME

Effect of Hole Diameter in Standoff Spacer

Tests in assembly 2.1 shown in Figure 2 with 0.086" spacing between the M55 detonator and the M219 lead cup 2 produced high order detonation of the lead explosive for holes with 0.055" diameter and larger. Above this diameter, the overall transit times were shorter than 0.936 microseconds (Table 5) and the witness discs were penetrated and spalled (Fig 13). Holes with 0.038" diameter and discs without holes under the detonator produced no detonations in the lead cups. The overall transit times were higher than 17.1 microseconds (Table 5) and the remains of the stop trigger switches were still visible on the undamaged witness discs (Fig 13).

In further tests, therefore, the standoff spacers with holes of 0.078" and 0.055" diameter were used. The steel washers were 0.061" thick and were strong enough so that the detonator output caused no spalling or fragments from the edge of the holes.

Effect of RDX Particle Size on Lead Initiation

Overall Transfer Times, Lead Cup No. 1

The results of tests conducted to find the influence of RDX particle size, loading pressure, and density are shown in Table 6. Table 7 contains the mean values of the overall transit times, the standard deviations of the means (σ_x) and the 90% confidence interval limits. From this table one can see that the overall transit times are related to the parameters as follows:

a. Longer for 11,000 psi than for 40,000 psi for class C and A RDX and not significantly different for class E RDX. Hence for class C and A, the loading pressure has a significant influence on the overall transit times, while for class E, this is not the case.

b. At 11,000 psi, no difference between RDX class C and A, and significant lower value for class E.

c. At 40,000 psi, no significant differences within RDX classes.

It should be noted that, at 11,000 psi, the loaded density of class E is much lower than that of the others, while at 40,000 psi all classes have about the same density. This may be due to the crystal strength being exceeded at the high pressure which, in all classes, leads to crushing to the extent that the final density and particle size distribution are not essentially different.

The effects of detonations in the lead on the witness disc correspond with the results of overall transfer time measurements. Figure 14 shows, for 11,000 psi, the witness discs of the two class C no-fires and of the first two tests each of class A and E. For 40,000 psi the witness discs from the first two tests are also shown. These results indicate only qualitative results since the penetration holes and the amount of spalling cannot be measured accurately. The visual findings (Fig 14), were used only to differentiate lead cup detonations from no-fires.

Calculated Excess Transit Time, Lead Cup No. 1

To further analyze the significance of the results, they were reduced to calculated excess transit times in the explosive lead as previously described. In essence, the constant subtracts from each overall transit time a constant representing the sum of ideal detonation transit time (t_{id}) through the lead explosive (Table 8) and either the time of flight of fragments (t_{frag}) or of shock (t_{shock}) across the gap ($L_1 = 0.0936"$, Table 1). Using fragment and shock velocities for M55 detonators of Lot LS-DZ-3347 described later (Table 24), the flight times are as follows:

$$t_{frag} = 573 \text{ ns}, \quad t_{shock} = 384 \text{ ns}.$$

The differences of overall transit times in Table 7, as described in the discussion of overall transit times, apply also for calculated excess transit times (Table 9). Since negative transit times, which are impossible, appear in the data with assumed fragment initiation, one is led to the conclusion that where negative values are shown, the particle size was small,

and initiation was caused solely by shock. The conclusion is that shock initiation dominates for high density compacts (which probably have small particle size because larger particles were crushed during loading) and for low density, small particle size compacts. It should be noted that the shock waves arrive before the fragments for the relatively small gap used. Hence fragment initiation implies that shock initiation did not occur but the shock may have sensitized the explosive. This may explain the smaller confidence interval and shorter calculated excess transit time for the two fragment initiation cases where large particle size, low density RDX was present.

Influence of Flyer Plates on Lead Initiation

Prior work by Smolen (Ref 9) had indicated that thicker closure discs on M55 detonators improved the ability of the latter to initiate leads over long standoff distances. Tests were conducted to determine if thicker closure discs would also improve the efficiency of transfer at the short standoffs commonly used in fuze trains.

Test of Closure Disc Thickness, Using a 0.104" Gap Distance

Aluminum flyer plates, 2 mil and 5 mil thick, were added to the 3-mil closure disc of the M55 detonator. Table 10 contains the test results. The three tests with 5-mil flyer plates gave no-fires of lead cup 3, indicated by the long overall transit times of 3.473 μ s and higher, and by the failure to produce evidence of detonation in the witness discs. The three tests, each with 2-mil flyer plates and no flyer plates, showed both detonations and no-fires of lead cup 3. The number of tests was too small to differentiate the influence of 2-mil flyer plates and that of the absence of any flyer plates. It can be concluded that the gap distance of 0.100" combined with the 0.055" diameter hole in the standoff spacer provides a marginal condition for initiation of lead cup 3 with the explosive Comp A5 (Table 3). For further flyer plate tests, therefore, the test assembly shown in 2.1 of Figure 2 was changed to reduce the detonator-lead distance to 0.041".

Tests of Flyer Plate Material Using a 0.041" Gap Distance

This section describes transit time tests made in a modified version of the test assembly shown in 2.1 of Figure 2. 5-mil flyer plates were added to the 3-mil closure disc of the M55 detonator Lot LS-229-3. The start of the transit time was triggered by the ionized shock wave of the detonator reaching the lead cup. The stop of the transit time was triggered at the base of the lead cup.

Table 11 contains mean values of the measured detonation transit times through the lead and the calculated excess transit times. The latter values were calculated by subtracting the ideal detonation transit time of the lead (302 ns) from the measured transit times. The values of 90% confidence level apply to both measured transit time and calculated excess transit time. They show that aluminum and steel flyer plates increase the transit and excess transit time values over that received in the absence of flyer plates by the same amount, and the copper flyer plate is even less effective than those of aluminum and steel. The superior performance without any added flyer plate indicates that the improved momentum transfer at longer distances, according to Smolen (Ref 9), was not obtained in the short distance tests. The data suggest that in this case the cause of initiation is shock, since the shortest excess transit times occurred with no added flyer plate.

Steel was the most effective additional 5-mil-thick flyer plate material, and this in spite of the observation that the fragments from aluminum travel fastest, those from steel slower, and those from copper are slowest, due to their increasing densities. From witness plates, it was found that the fragments from steel are larger, which appeared to compensate for their lower velocity compared with aluminum.

Initiation of Lead Cups No. 2, 3, and 4

The sensitivity to initiation of lead cups No. 2, 3, and 4 was compared in tests using test assembly shown in 2.1 of Figure 2. The results were obtained by firing through a 0.055" hole. They are shown in Table 12. Lead cup No. 3 loaded with the explosive Comp A5 (Ref 10) had two no-fires in three tests, indicated by excessively long overall transit times of 5.229 and 5.925 μ s and low order detonation effects on the witness discs. Lead cups No. 2 and 4 were different in the granulation of RDX: Lead cup No. 2 contained RDX, Type B, class G (Fig 8.4), while lead cup No. 4 was pressed with RDX without the fine fraction smaller than 149 microns (footnote 7 to Table 3). This difference in granulation, however, produced no difference in the overall transit times at the 90% confidence interval limits. There was a difference with the 0.078" dia hole as will be described later in this report.

The low sensitivity of lead cup No. 3 can be explained by the explosive Comp A5 having less sensitivity than composition RDX/graphite (99.5/0.5) used in lead cups No. 2 and 4. The relatively long spacing

of $L_3 = 0.1043$ " constitutes, because of the short length of the lead cup an additional unfavorable factor for this case. The lack of a significant difference in sensitivity between lead cups No. 2 and 4 led to another series of tests with an increase to 0.078" diameter of the hole in the standoff spacer. The overall transit times for the larger hole are shown in Table 13. The mean values for overall transit times for lead cup No. 4 are, at the 90% confidence interval, significantly higher than those for lead cup No. 2. To further consider the significance of the results, the overall transit times were reduced to calculated excess transit times in the explosive lead. The times subtracted for travel of shock and fragments are listed in Table 14, the calculated excess transit times in Table 15. The results can be summarized as follows:

a. With a 0.055" diameter hole, the calculated excess transit time for assumed fragment initiation is longer for lead cup No. 2, loaded at Picatinny Arsenal with 99.5% RDX graphite containing 50 μ average particle size RDX than it is for lead cup No. 4, loaded at Lone Star with the same mixture as above, except for the average particle size of the RDX being 220 μ .

b. Since negative transit times are impossible, it can be assumed that, where negative values appear in test series with a 0.078" diameter hole, initiation was by shock, not by fragments. This applies especially to lead cup No. 2.

c. The change in the size of the hole from 0.055" to 0.078" diameter has, within the 90% confidence interval of the mean to t_{trans} , no influence on the fragment initiation of lead cup No. 4.

It follows from the lower excess transit time that lead cup No. 2 shows more sensitivity to shock than lead cup No. 4. This is considered to be associated with the content of the fine-particle fraction in the class G RDX increasing the sensitivity to shock initiation. It should be noted that the explosive of lead cup No. 4 does not contain RDX smaller than 149 microns (sieve No. 100). Fragment initiation of lead cup No. 4 includes the possibility that the shock may have sensitized the explosive, as mentioned before. Short calculated excess transit times for fragment initiation of lead cup No. 4 and longer values for shock initiation of lead cup No. 2 in test assemblies with 0.078" diameter holes in the standoff spacer might, therefore, be explained by the sensitizing action on the explosive of the prior shock.

Influence on Detonation of the Covering of the Lead

The finding of an eccentric coining in the bottom in one of 50 lead cups No. 3 (Fig 15) was the reason for tests in which the thickness of the covering on the lead was varied between 2 and 10 mils. Tests were started with lead cup No. 3 in the test assembly shown in 2.2 of Figure 2. The M55 detonator output passed through a 0.055" diameter hole of the standoff spacer and had a spacing distance of 0.1261" from the covering of the lead. The test results are shown in Table 16. The 10-mil aluminum foil caused no-fires as indicated by overall transfer times of 2.607 μ s and higher, and by small effects on the witness discs. Tests with 5 mil, 2 mil, and no foils showed lead detonations with nominal effects on the witness discs, and relatively long overall transfer times. No differences between the three were observed. Three additional tests with the same spacing but with reversed lead cups No. 3 in the test assembly shown in 2.3 of Figure 2 did not improve the results (see Table 16).

Tests were then conducted with lead cup No. 4, where the coin covered an area of almost the whole inner diameter. The results of tests with reduced spacings are shown in Table 17. The spacing distance of about 0.100" was, however, still in the range where no-fires and uncertain initiations happened. This applied even for lead cup No. 4 where the explosive RDX/graphite (99.5/0.5) is more sensitive than the explosive Comp A5 of lead cup No. 3. It can be concluded that the thick aluminum covering of 10 mils obstructs the initiation under marginal conditions. To obtain reliable overall transfer times, the spacing has to be reduced. Further tests varying the thickness of the lead covering and measuring the DEE are described later in this report.

USE OF THE DETONATION ELECTRIC EFFECT FOR LEAD INITIATION STUDIES

The DEE was first investigated by Travis (Ref 11) in liquid explosives, and then by Hayes (Ref 12) in solid explosives. This effect provides an electrical signal associated with the ionization produced as the detonation wave front progresses through the explosive. In order to utilize this approach for measurement of initiation of lead cup explosives, considerable effort was required to eliminate electrical disturbances associated with the small dimensions.

Circuit Diagram for t_{OT} and DEE

The circuit diagram for measuring the overall transfer time (t_{OT}) and the DEE is shown in Figure 19. The DEE pickup, an iron cylinder of 0.143" diameter and 0.165" high, was connected to the 7A11 amplifier of a 7904 Tektronix oscilloscope. The 7A11 amplifier has a remote field effect transistor (FET) probe with an input impedance of 1.2 pF and 1 megohm included. This was used to minimize the distance from the sample to the probe (a nominal distance of 10 inches was used in our test). In addition, the sample was shielded from external signals by the firing enclosure (metal cylinder), which acted as a Faraday cage, and by the grounded covering of the lead. For tests with lead cups (Fig 18.2 and 18.3) the cups were grounded. The electrical disturbance from the M55 detonator was small because it was initiated, not electrically, but by a stab needle. The oscilloscope sweep was externally triggered when the start switch on the bottom edge of the detonator closed (Fig 19). Completion of lead detonation activated the stop switch of the time interval meter at the edge of the DEE pickup corresponding with position 1 of switch No. 1 in Figure 4. The pin switch circuit between signal sources and time interval meter is shown in Figure 5.

DEE Profile

The DEE profile is shown schematically in Figure 20. The signal of the start trigger switch is abruptly damped down at the time t_{shock} when the ionized shock wave from the detonator reaches the grounded covering of the lead. The fragments from the detonator closure disc reaching the covering of the lead at the time t_{frag} caused a new oscillation of the DEE signal. At the time t_{det} high-order detonation began. From this point, the slope of the curve increased steadily; it ended at the time t_{end} when the detonation reached the pickup. The time t_{end} which is the overall transfer time, was simultaneously measured with a time interval meter as described before. The signal to the right of t_{end} in Figure 20 is the signal of the stop switch. Representative records of lead explosive No. 5 and of the inert Pentek (pentaerythritol) filling in test assembly 18.1 shown in Figure 18 are given in Figure 21. The time scale from zero to t_{frag} , i.e., up to the time when fragments arrive at the lead covering, could be evaluated for leads with explosive and inert filling in the same manner. In the preliminary tests, the time scale was measured with the approximate accuracy of the graticule image on the oscillograms. The data are indicated as R-values. In the main tests, a magnifying glass with a micrometer scale was used to increase accuracy. These values were, in most cases, referred to as M-values.

RESULTS: USE OF THE DEE FOR LEAD INITIATION STUDIES

Overall Transfer Time From DEE Profile and Time-Interval Meter

To check the accuracy of DEE measurements against that of the time interval meter, the overall transit times measured in tests No. 166 to No. 180 were compared. In Figure 22 are plotted, for both methods of measurement, the mean values and their 90% confidence intervals vs the thickness of the covering of the lead. The overall transit times in Figure 22 increase with the thickness of the foil on top of the lead explosive No. 5 (Fig 18.1). The agreement of mean values from DEE profiles and time-interval meter measurements is good when the difference in source of signal pickups for the stop and the 90% confidence intervals are taken into account. The start switch position has no influence on the two measurements since both starts are triggered with the same impulse.

Influence of Foil Thickness on Calculated Excess Transit Times

The mean values of calculated excess transit time in Table 22 are calculated from overall transit time by subtracting time for fragment travel (including passage through the covering) and also ideal detonation transit time through the thickness of the lead (Table 21). This data shows a trend of increase of the calculated excess transit time with the foil thickness. The increase is, however, not significant at the 90% confidence limits of the means. The measured increase of the overall transit times seems to be caused mainly by the increase of travel time of the fragments with the foil thickness (Table 20). Referring to no-fires in previous tests with 10-mil-thick foil (Table 16), it can be expected that increased precision of measurements could show a relation between calculated excess transit time and thickness of covering.

Shock Wave and Fragment Velocities from DEE Measurements

The times of shock wave and fragment travel across the gap distance between detonator bottom and lead covering were used to calculate their velocities. Variations of the foil thickness on the lead explosive had shown that travel times of fragments include the time for penetration of the lead covering, while the lead covering had no influence on the travel time of the shock wave (Table 20). The data in Table 24 used for the .0068" gap a foil thickness of 0.005", and for the 0.091" gap a lead cup covering of 0.0053" (lead cup No. 4, Table 2). The data for the 1.000" gap measured by Voreck (Ref 13) used a 0.020" thick foil on top of the stop switch at the end of the fragment travel. Travel times for shock wave and fragments in

the DEE profiles were the most reliable values. Measurements in the DEE test assembly with lead cups shown in Figure 18.2 were, therefore, evaluated only for velocities (Table 24). In Table 25, mean velocities and their 90% confidence level are listed in relation to varied gap distances for M55 detonators of the Lot LS-DZ-3347 and the Lot IOP-1-74. The results for the three gap distances are as follows: For the 0.091" gap at the 90% confidence level the two lots gave significantly different fragment velocities, but not shock velocities. The other effect found significant at the 90% confidence level were: The increase in fragment velocity for Lot IOP-1-74, as the gap was decreased from 0.091" to 0.068", and for Lot LS-DZ-3347 for a decrease from 1.000" to 0.091". The numerical values indicate that large changes of the gap such as the above produce only small changes in fragment velocity.

Influence of Detonator on Lead Initiation

Two lots of M55 detonators were compared as to their ability to initiate lead cups (type No. 4). The overall transfer times measured with the time-interval meter in previous tests (Table 13) and simultaneously by the DEE profile (Table 22) were used to determine calculated excess transit times of lead cups. The standoff spacer had a hole of 0.078" diameter, and the gap distance between the bottom of the M-55 detonators and the covering of the lead cup was 0.098". Tests No. 126 and 131 were conducted in test assembly 2.1 shown in Figure 2 with stop trigger switch No. 2 (Fig 4). Tests No. 144 and 148 and No. 158 to 168 were run in test assembly 18.2 shown in Figure 18 with stop trigger switch No. 1 in Position 1 (Fig 4). Table 25 shows the influence of M55 detonators, Lot LS-DZ-3347 and Lot IOP-1-74, on the calculated excess transit times. It can be concluded that the M55 detonators of Lot LS-DZ-3347 initiate lead cup No. 4 better than those of Lot IOP-1-74. The values of tests No. 126 to 131 differ a little from those listed in Table 15 since the latter were calculated with mean times of ideal detonation (t_{id}) instead of individual values (Table 25). The values in Table 25 were obtained under equal conditions, with the different positions and the makeup of the stop switch being neglected. Detonators of Lot LS-DZ-3347 caused lead cup No. 4 initiations predominantly by fragments. Since the two negative values are impossible, shock initiation can be assumed in these cases. In cases of low calculated excess transit time for assumed fragment initiation, the previous shock wave through the lead explosive will have facilitated the initiation by fragments that followed. The longer calculated excess times and the one no-fire of lead cup No. 4 in 5 tests with detonators of Lot IOP-1-74 go along with the

lower velocities of shock and fragments compared with the values of Lot LS-DZ-3347 detonators (Table 22). The scattering of values in tests No. 144 to 148 may be due to the edge location of the stop switch since these were the first tests with it.

Replacement of M55 Aluminum Foil Closure with Teflon/Paper

The tests with detonators of Lot KN-E-26, closed with a Teflon/paper laminate, were run to check the influence of missing fragmentation in this case. Data are given in Table 22. Since test No. 148 with a 0.0908" spacing gave a no-fire, the standoff spacer, 0.061" thick, was reduced to a thickness of 0.035" to get the smaller spacing of 0.0648". The results of this test series (tests No. 150 to 154) are summarized as follows:

a. The DEE records show an absence of the fragment arrival pulse that occurs with aluminum closure discs of standard detonators.

b. The travel times for shock (Table 22) give a higher shock velocity (Table 23) than that for M55 detonators with aluminum closure discs. From these results can be concluded that the arrival of fragments at the lead cup is accurately indicated when detonators with aluminum closure discs are used, since Teflon/paper fragments do not have a fragmentation effect and, therefore, give no indication in the DEE profile. The increase in shock velocity by the replacement of the aluminum closure disc with a Teflon/paper laminate corroborates the results of flyer plate tests (Table 11) that showed the shortest calculated excess transit time when the flyer plates were left out. In the test series with M55 detonators of Lot KN-E-26 the replacement of the aluminum closure disc by the Teflon/paper laminate followed the trend established by the absence of flyer plates in the tests described before.

CONCLUSIONS

For testing the detonation transfer from M55 detonators to lead cups across short spacings, test assemblies were developed for measuring over-all transit times and DEE profiles. The time-interval meter used in combination with a pin switch circuit as shown in Figure 5 provided time values accurate to 1 nanosecond. The capacitive pickup for DEE measurements was connected to a remote field effect transistor probe of the amplifier of the oscilloscope to minimize electrical disturbances. The time data obtained by time interval meter or DEE measurements served for calculating excess transit times of the detonation through the length of the lead explosive to

compare influences of variation in detonators and lead cups on the detonation transfer. DEE records also allowed measurement of fragment and shock velocities from detonators, and determination of whether initiation occurred by shock or by a combination of shock and fragments. In the first tests both shock and fragments of the detonator output were attenuated to simulate the effect of marginal donor conditions in the train.

The lead cup explosive RDX/graphite/Calcium Resinate (99.00/0.65/0.35) was predominantly initiated by shock instead of fragmentation when the RDX particle size was reduced and when the loading pressure was increased. The lead explosive RDX/graphite (99.5/0.5) in M219 lead cups showed an equivalent behavior. Lead cups with class G RDX containing fine particles (loaded at Picatinny Arsenal) were more sensitive to shock initiation than those with RDX whose fine particle fraction (smaller than 149 microns) had been removed. At the short spacings used, the effect of the detonator output was reduced with increasing thickness of flyer plates; however, the replacement of aluminum flyer plates by paper reduced the output still more drastically. In addition, the effect of output was reduced by flyer plates of copper more than by those of aluminum and steel. As to lead explosives, Comp A5 was found to be less sensitive to initiation than RDX/graphite (99.5/0.5). In M42 grenade lead cups, and eccentric coin was found. This phenomenon could become the cause of duds, since fragments would have to penetrate thicker foil in the noncoined area. Tests with varied thicknesses of covering on the lead to simulate this condition showed that the 10-mil foils increase the number of duds when the detonator output is minimized. Tests with nonattenuated detonator output also showed a trend toward increase in the calculated excess transit time with foil thickness. From calculated excess transit time in M219 lead cups (Lone Star) it can be concluded that M55 detonators from Lone Star (Lot LS-DZ-3347) cause initiation more readily than those of IOP (Lot IOP-1-74). This result corroborates the significance of the velocities of fragments, which are higher for Lone Star than for IOP.

Tests with M55 detonators closed with a Teflon/paper laminate replacing the aluminum closure disc resulted in a DEE profile without fragment signals. Furthermore, the shock velocity was higher than that of standard M55 detonators. These two results support the findings in flyer plate tests and confirm that fragments from closure discs of aluminum cause real signals in the DEE profile. Measurements of DEE profiles provide a significant addition to the ability to study details of detonation transfer compared with previous methods such as flash X-rays and high speed cameras (Ref 4).

Tests with variations in M-55 detonators (described in the Appendix) showed that the present design is optimum for short gaps (less than 0.1 inch), and that initiation of the acceptor was due to both blast and fragments at short spacings. Thicker closure discs increased fragment energy but decreased shock or blast. Prior studies had indicated that thicker closure discs would increase ability to initiate over longer gaps where blast is no longer a factor (Ref 9).

REFERENCES

1. Dixon, W. and Massey, F. *Introduction to Statistical Analysis*, Pages 109-123, McGraw Hill, 1969
2. Voreck, W. E. and Dalrymple, E. W., *Development of an Improved Stab Sensitivity Test and Factors Affecting Stab Sensitivity of M55 Detonators*, Picatinny Arsenal Technical Report 4263, June 1972
3. US Specification MIL-D-14978 A (MU), *Detonator, Stab, M55*, 30 October 1972
4. US Specification MIL-R-398 C (2), Table II, 28 April 1971
5. Stott, B. A. and Koch, L. E., *Optimization of Filler Size Distribution for Preparing Castable Plastic - Bonded Explosives*, NWC-TP-5216, Naval Weapons Center, China Lake, California, May 1972
6. Hutchinson, R. W., *Use of Liquid Sedimentation Technics for Measuring the Particle Size Distribution of Primary Explosives*, Picatinny Arsenal Technical Report 4387, November 1972
7. TIGER Computer Program Documentation (W. E. Wiebenson, Jr., W. H. Zwisler, L. B. Seely, Stanford Research Institute, Menlo Park, California, and S. R. Brinkley, Jr.), Combustion and Explosives Research Inc., Pittsburg, Pennsylvania), November 1968
8. Ramsay, J. B. and A. Popolato, *Analysis of Shock Wave and Initiation Data for Solid Explosives*, Proceedings, Fourth Symposium (International) on Detonation, October 12-15, 1965, pages 233/238, Superintendent of Documents, U. S. Government Printing Office, Washington, D. C., 20402

9. Smolen, S., *M55 Detonator Test*, Test Report, 3 February 1971
10. Fedoroff, B. T. and Sheffield, O. E., *Encyclopedia of Explosives and Related Items*, Picatinny Arsenal Technical Report 2700, Vol 3, page C476, C477, Comp A5, Dover, N. J., 1966
11. Travis, Jr. R., *Electrical Transducer Studies of Initiation of Liquid Explosives*, 4th Detonation Symposium, page 609/615
12. Hayes, B, *The Detonation Electric Effect*, Journal of Applied Physics, 38, NO. 2, 507-511, February 1967
13. Voreck, W. E., *Detonator Output Measurement by Fragment Velocity*, Minutes of Department of Defense Fuze Engineering Standardization Working Group, April 1973
14. Schwartz, F., Slagg, N., Dalrymple, E., Millington, L., and Voreck, W., *Detonation Transfer*, Picatinny Arsenal Technical Report 4570, December 1973

Table 1

Spacings (L) between detonator and lead cup

Lead Cup No.	Designation	t_{OT} Standoff		
		Test Assemblies (Fig 2)		
		2.1	2.2	2.3
1	L_1	0.0936	-	-
2	L_2	0.0864	-	-
3	L_3	0.1043	-	-
3	L'_3	-	0.1261	0.1261
4	L_4	0.0908	-	-
4	L'_4	-	0.1261	0.1261
4	L''_4	-	0.0981	0.0981
4	L'''_4	-	0.1016	-

DEE t_{OT} Standoff

Lead Cup No.	Designation	Test Assemblies (Fig 18)		
		18.1	18.2	18.3
4	L_4	-	0.0908	-
4	L'''_4	-	-	0.0883
5	L_5	0.0680	-	-

Table 2

Lead cup, dimensions and types

Description	Designation ^a	Lead Cup (LC) ^a (inches)				
		No. 1	No. 2	No. 3	No. 4	No. 5
	SK-BP-123	M219, PA	M42, LS91-12	M219, LS95-10	Nylon Washers	
Cup, OD	D	.2018	.1736	.1724	.1738	.5000
Coined area, D	D _C	.1450	.1174	.0770	.1151	
Cup, ID	D _I	.1853	.1341	.1551	.1317	.1470
Flange, OD	D _{FL}	.2472	.2259	.2473	.2268	
Coined bottom thickness	A	.0042	.0051	.0049	.0053	.0020
Bottom rim thickness	B	.0116	.0099	.0087	.0111	.0050
Flange thickness	C	.0067	.0059	.0096	.0066	.0100
Average bottom thickness	X	.0071	.0062	.0078	.0067	X=A=B
Total height	α	.1078	.1142	.1008	.1110	.1270 ^b
Explosive plus bottom height	h'	.1038	.1098	.0979	.1054	
Average explosive height	h	.0967	.1036	.0901	.0987	.1205

^aSee Figure 7

^bThickness of the nylon confinement

Table 3

Lead cup explosives, components

Lead Cup No.	Explosive Compositions			
	RDX (%)	Stearic Acid ^a	Lubricants	
			Graphite ^b	Ca-resinate ^c
1	99.00 ^d		.65	.35
2	99.50 ^e		.50	
3	min 98.50 ^f max 99.00 ^f	min 1.00 max 1.50		
4	99.50 ^g		.50	
5	99.50 ^h		.50	

^aStearic acid, MIL-A271

^bGraphite, flake, MIL-G-155D, Grade I

^cCalcium-resinate MIL-C-20470A, Type II

^dRDX, MIL-R-398C, Type B, Class C, A, and E, see Fig 8.1-8.3

^eRDX, Type B, Class G, Lot HOL-27-6

^fComposition A5, Ref 10

^gRDX, Type B, Class C through 30 mesh (595 microns), on 100 mesh (149 microns)

^hRDX, MIL-R-398C, Type B, Class A, see Fig 8.2

Table 4

Density vs loading pressure for lead cup explosives

No.	Lead Cup		Weight (g)		Density (g/ml) ^b
	RDX class ^a	Pressure kPSI	Empty cup	Explosive	
1	C	11	.038	.068	1.62
		40		.072	1.73
	A	11		.069	1.60
		40		.073	1.73
	E	11		.061	1.48
		40		.069	1.70
2		11	.054	.042	1.74
3		10.5	.032	.050	1.75
4			.054	.039	1.74 ^c
5	A	10		.054	1.63
	Pentek ^d	10		.041	1.22

^aSee Figure 8.1-8.3

^bValues determined with measured weights and dimensions

^cValue, determined by buoyancy in water and averaging five measurements, was d = 1.71 g/ml

^dPentek (Pentaerythritol) as inert material in blanks

Table 5
Effect of reduced donor source areas on overall transfer times

Fraction of 0.11" Dia Impact Area	Hole Diameter (inches)	Overall Transfer Times (nanosec)		Test No.	Remarks	
		Individual	Average			
1	0.110	848;	757	802	22, 23	Explosive detonated
1/2	0.078	859;	768	813	24, 25	Explosive detonated
1/4	0.055	936;	881	908	26, 27	Explosive detonated
1/8	0.038	17,100;	4,100		30, 31	Explosive burned
0	0.000	59,600;	48,500		28, 29	No reaction

NOTES:

Variable was hole diameter in standoff spacer, part No. 6, test assembly 2.1 in Figure 2, standoff 0.086"

Donor: M-55 detonator, Acceptor: M219 Lead Cup
 Lot LS-DZ-3347 OA #8833562

Table 6

Overall transit times for RDX classes C, A, and E

Test Assembly: Fig 2.1, $1_1 = 0.094$; Fig 2.1, item 6 with hole .055 dia
 Detonator: M55, Lot LS-DZ-3347
 Lead cup type: Table 2, No. 1
 Variable: For grain size of RDX class A, C, E, see Fig 8.1 - 8.3; for density (loading pressure), see Fig 10

	Class C		Class A		Class E	
	11 KPSI time (ns)	40 KPSI time (ns)	11 KPSI time (ns)	40 KPSI time (ns)	11 KPSI time (ns)	40 KPSI time (ns)
26	917 ^a	832	917	854	872	776
	7657 ^a	778	983	741	903	784
	943	875	928	860	974	748
	932	876	928	769	901	888
	976	823	955	792	799	961
					862	898
					931	936
					799	920
					892	889
					934	(440)

^a See Fig 14, Tests No. 34 and 35: no penetration of the witness disc because of no lead cup detonation

Table 7

Experimental data on effect of RDX particle size and density in lead on initiation^a

Loading pressure (psi) RDX class	11000			40000		
	C	A	E	C	A	E
Mean particle size (microns)	498	224	22,74	498	224	22,74
Pressed density (g/cm ³)	1.62	1.60	1.48	1.73	1.73	1.70

		Overall Transit Times (ns)	
No. of tests	n	3 ^b	5
Mean value	\bar{x}	950	942
St Dev of mean	$\sigma_{\bar{x}}$	13	12
90% Upper confidence limit of mean		972	962
90% Lower confidence limit of mean		928	922
			858
			807
			803
			867
			23
			841
			765
			825
			10
			867
			26
			909
			825

^a Donor was an M-55 detonator. The gap was 0.094". Explosive in lead was 0.100" thick, 0.185" diameter, and exposed on surface closest to M-55. The composition was RDX/graphite/Ca-resinate (99/0.6510.35)

^b There were also two no-fires, omitted from further calculations

Table 8

TIGER code calculated ideal detonation time

Ideal detonation transfer time (t_{id}) for lead cup No. 1

Density g/cm ³	V_D^a mm/ μ s	t_{id}^b ns
1.48	6.065	417
1.60	7.030	360
1.62	7.190	352
1.70	7.830	323
1.73	8.070	313

^a V_D for lead explosive RDX/graphite/Calcium-resinate (99.00/0.65/0.35) (Fig 11)

^b $t_{id} = h'/V_D$; $h' = h' - A = 0.0996''$ (Table 2)

Table 9

Calculated excess transit times

Loading pressure (psi) RDX class	11000			40000		
	C	A	E	C	A	E
Mean particle size (microns)	498	224	22,74	498	224	22,74
Pressed density (g/cm ³)	1.62	1.60	1.48	1.73	1.73	1.70
$t_{cal, fr}$ - Fragm init assumed (ns)	25	9	-103	-49	-83	-29
$t_{cal, sh}$ - Shock init assumed (ns)	214	198	86	140	106	160
90% Confidence interval of mean (ns)	±22	±20	±29	±30	±38	±42

NOTE:

Calculated mean values of overall transit times obtained by subtracting time for shock or fragment travel and also subtracting ideal detonation transit time through the thickness of the lead. For overall transit times see Tables 6 and 7; for ideal detonation transit times see Table 8.

Table 10

Overall transit times for varied thicknesses of flyer discs

Test assembly: Fig 2-2.1, item 6, $l_3 = .1043"$, hole = .055" dia
 Detonator : M55, Lot LS-DZ-3347
 Lead cup type: Table 2, No. 3
 Variable : Thickness "e" of flyer disc, placed against output
 face of M55 (located between items 5 and 6, Fig 2).

Test No.	e (in.)	time (ns)	Remarks
74	.005	7227	Residue of LC explosive } No traces LC explosive burned } of detona- tion in WD
75		3473	
76		4459	
77	.002	918	WD penetrated, LC explosive detonated
78		858	
79		1146	Depression in WD, no detonation
95	no	5229	WD depressed
96		1043	Spalling of WD with small hole
97		5925	Residue of LC explosive

Table 11

Influence of flyer plates on calculated excess transit times in lead explosives^a

Flyer Plate	Mean lead transit time (ns)	Number of tests	90% CL of means	Mean calculated excess transit time (t_{cal}, ns)
None	392	10	7.6	90
5 mil Aluminum	480	6	21.2	178
5 mil Steel	466	5	33.9	164
5 mil Copper	566	5	28.3	264

^aM-55 detonator in an M42 Grenade diecast washer with a 0.041" gap distance to the lead cup. The lead cup (Dwg 8833562) was loaded with RDX/graphite (99.5/0.5) at 11000 psi. A density of 1.742 g/cm³ was obtained, with an explosive charge 0.100" thick and 0.175" diameter.

Table 12

Overall transit times of lead cups No. 2, 3, and 4, hole .055" dia

Test Assembly: 2.1 in Fig 2 with standoff L according to LC No. 2, 3, and 4; for thickness of covering A see Fig 7 and Table 2, also item 6 in Fig 2, with .055" dia hole (standoff spacer)

Detonator: M55, Lot LS-DZ-3347

Variables: Dimensions of LC, explosive of LC (see Table 2)

Lead Cup No. 2
 $L_2 = .0864, A = .0051$ in.

Lead Cup No. 3
 $L_3 = .1043, A = 0.0049$ in.

Lead Cup No. 4
 $L_4 = .0908, A = 0.0053$ in.

time (ns)	Remarks	time (ns)	Remarks
909 } 958 }	WD ^a penetrated	5229	WD depressed
966	Spalling of WD, with small hole	1043	Spalling of WD, with small hole
944 ± 29 ^b		5925	Residue of LC explosive
		894	Spalling of WD, with small hole
		884	
		919	
		899 ± 17 ^b	

^aWD: witness disc

^bMean ± 90% confidence interval

Table 13

Overall transit times of M219 lead cups No. 2 and 4

Barrier hole: .078" dia
 Test assembly: 2.1 in Fig 2, also item 6 in Fig 2, with .078" dia hole
 Detonator: M55, Lot LS-DZ-3347
 Variables: Dimensions of LC (Table 2)

Lead Cup No. 2 $L_2 = .0864", A = 0.0051"$			Lead Cup No. 4 $L_4 = .0908", A = 0.0053"$		
Test No.	Time (ns)	Remarks	Test No.	Time (ns)	Remarks
24	768	} WD penetrated	126	908	WD penetrated
25	859		127	820	} Spalling of WD, center cracked
132	902		128	901	
133	784		129	881	} WD penetrated
134	733		130	883	
135	758		131	900	
	801 ± 43.9^a			882 ± 21.7^a	
	26.7			13.2	

$\sigma_{\bar{x}}$

^a Mean \pm 90% confidence interval

Table 14

**Travel times of shock and fragments for M55 detonator, Lot LS-DZ-3347^a
and ideal detonation times of used cups No. 2 and 4^b**

Cap distance (in.)	Time (in ns)	
	t_{frag}	t_{shock}
0.0864	529	354
0.0908	555	372
0.0981	600	402
0.1016	622	416
0.1261	771	517

^a $v_{\text{frag}} = 4.152 \text{ mm}/\mu\text{s}$

from Table 23

$v_{\text{shock}} = 6.197 \text{ mm}/\mu\text{s}$

^bIdeal detonation times for lead cups No. 2 and 4 differ because of different thicknesses of the explosive charge:

LC No. 2 with 0.105" thick charge: 313 ns

LC No. 4 with 0.100" thick charge: 299 ns

Analogous explosive data are: RDX/graphite (99.5/0.5), density 1.74 g/cm³, and ideal detonation velocity of 8.504 mm/ μ s (see Fig 11)

Table 15

Calculated excess transit times (in nanosec) for lead cups No. 2 and 4
in test assembly shown in 2.1 of Figure 2

<u>0.055" diameter hole in standoff spacer (see Table 12)</u>		No. 2	No. 4
$t_{cal,fr}$	fragment initiation	67	40
	assumed	116	30
		124	65
Mean $t_{cal,fr}$	102	45	
90% confidence interval of mean	±29	±17	
<u>0.078" diameter hole in standoff spacer (see Table 13)</u>		No. 2	No. 4
$t_{cal,fr}$	fragment initiation	-74	54
	assumed	17	-34
		60	47
		-58	27
		-109	29
		-84	46
$t_{cal,sh}$	shock initiation	101	237
	assumed	192	149
		235	230
		117	210
		66	212
		91	229
Mean $t_{cal,fr}$	-41	28	
Mean $t_{cal,sh}$	134	211	
90% confidence interval of mean ^a	±44	±22	

^aApplies to both $t_{cal,fr}$ and $t_{cal,sh}$

Table 16

Overall transit time for varied foil thicknesses on lead cup No. 3

Test assemblies: 2.2 and 2.3 of Fig 2, standoff $L_3' = .1261$,
 item 6, with .055" dia hole for 2.1 of Fig 2
 Detonator: M55, Lot LS-DZ-3347
 Lead cup type: No. 3, M42, LS 91-12
 Variables: Foil thickness f , bottom $A = f$

Test Assembly 2.2, Fig 2 foil on top of LC-flange			Test Assembly 2.3, Fig 2 LC-bottom "A" as foil "f"			
f (in.)	Time (ns)	Remarks	f (in.)	Time (ns)	Remarks	
.010	5691	Residue of LC explosive	.005	1065	WD penetrated	
	17231			WD depressed	1290	WD depressed
	2607	LC explosive burned			975	Spalling of WD
.005	1838	WD depressed		.002	1939	WD depressed
	1963				Spalling of WD	1517
no foil	1215	Spalling of WD		no foil		1840
	1341	Spalling of WD	1313		Spalling of WD	
						1313

Table 17

Overall transit time for varied foil thicknesses on lead cup No. 4

Test assemblies: 2.2 Fig 2, standoff $L_4''' = .1016''$, AL foil .136" dia on explosive $L_4' = .0981''$, $L_4 = .1261''$, item 6, Fig 2, with .055" dia hole
 Detonator: M55, Lot LS-DZ-3347
 Lead cup type: No. 4
 Variables: 1) Foil thickness f (in assembly 2.3, Fig 2, LC bottom A as foil f)

Test assembly 2.2, Fig 2 standoff $L_4''' = .1016$ (in.)			Test assembly 2.3, Fig 2 standoff $L_4' = .0981$ (in.)		
f (in.)	Time (ns)	Remarks	f (in.)	Time (ns)	Remarks
.0020	1563	Spalling of the WD, similar in	.0053	1075	Beginning of spalling
	1410			933	
	914		3801 ^a	LC expl burned	
	863				
1095	952	Spalling of WD			
			937	WD penetrated	
			Standoff $L_4 = .1261$ (in.)		
			.0053	1270	WD
				1346	depressed

^aNo-fire

Table 18

Nylon washer lead No. 5, time measurements from DEE-profile

Test Assembly: 18.1 in Fig 18; $L_5 = .0680"$, item 6 in Fig 18, with
.250" dia hole

Detonator: M55, Lot IOP-1-74

Variable: Aluminum foil over acceptor, item 7, Fig 18

Test No.	Foil (mil)	Time (nanoseconds) ^{a, b}					Detonation Effect
		t_{shock}	t_{frag}	t_{det}	t_{end}	t_{OT}	
171	2	299	381	476	878	864	Yes
172		251	476	551	911	889	Yes
173		320	456	599	939	933	Yes
174		286	408	585	864	884	Yes
175		313	497	667	932	916	Yes
166	5	354	510	741	959	(1043)	Yes
167		286	456	510	912	889	Yes
168		279	442	741	932	923	Yes
169		313	476	660	966	979	Yes
170		279	469	469	912	901	Yes
176	10	272	537	694	1054	1025	Yes
177		327	517	694	1027	1007	Yes
178		272	469	612	980	936	Yes
179		313	476	646	939	943	Yes
180		306	497	694	993	988	Yes

^a DEE = time scale measured with magnifying glass

^b For illustration of DEE vs time, see Fig 20; for oscillogram, see Fig 21

Table 19

Lead No. 5, Inert acceptor transit time measurements from DEE-profile

Test Assembly: 18.1 in Fig 18; $L_5 = .0680''$, item 6 in Fig 18, with
.250" dia hole, item 8 in Fig 18.1; replaced by
Pentek (inert)

Detonator: M55, Lot IOP-1-74

Variable: Aluminum foil, item 7, Fig 18.1

Test No.	Foil (mil)	Time (nanoseconds) ^{a, b}				Remarks
		t_{shock}	t_{frag}	t_{end}	t_{OT}	
187	2	314	537	>2000	2618	
188		314	483		2112	
189		273	503		2617	
184	5			>2000	2380	} Failure of camera
185					2210	
186		314	510		2628	
181	10	348	498	>2000	2308	
182		307	505		2658	
183		348	544		2891	

^a DEE, time scale measured with magnifying glass

^b For illustration of DEE vs time, see Fig 20; for oscillogram, see Fig 21

Table 20

Mean times and velocities for shock and fragments of M55 detonator, lot IOP-1-74, across a gap of 0.068"^a

Foil (mil)	Number of tests	\bar{t}_{shock} (ns)	\bar{t}_{frag} (ns)	\bar{v}_{shock} (mm/ μ s)	\bar{v}_{frag} (mm/ μ s)
RDX/Graphite (99.5/0.5) ^b					
2	5	293±20	444±35	5.923±0.434	3.932±0.324
5	5	302±24	471±19	5.764±0.417	3.679±0.143
10	5	298±18	499±21	5.829±0.363	3.469±0.143
Pentek (pentaerythritol) inert ^b					
2	3	300±23	508±26	5.776±0.453	3.409±0.172
10	3	334±23	516±24	5.184±0.364	3.354±0.149

^aFor means and their 90% confidence intervals of values, see Tables 18 and 19

^bFillings of lead No. 5 as acceptor

Table 21

Excess transit times for nylon washer lead No. 5
with coverings of 2, 5, and 10 mil Al foil

Test No.	Aluminum foil over explosive (mil)	Measured transit time ^a trans (ns)	Explosive height h (in.)	Ideal detonation t _{id} (ns)	Excess transit time t _{cal} (ns)
171	2	497	.1271	398	99
172	2	435	.1259	395	40
173	2	483	.1169	366	117
174	2	456	.1217	381	75
175	2	435	.1129	354	81
Mean					82
σ					13
90% C.L.					21
166	5	449	.12 ^C	376	73
167	5	456	.12 ^C	376	80
168	5	490	.12 ^C	376	114
169	5	490	.1197	375	115
170	5	443	.1192	374	69
Mean					90
σ					10
90% C.L.					17
176	10	517	.1172	367	150
177	10	510	.1304	409	101
178	10	511	.1253	393	118
179	10	463	.1166	365	98
180	10	496	.1299	407	89
Mean					111
σ					11
90% C.L.					18

^a Calculated with data from Table 18

^b $t_{id} = h/v_D$; $v_D = 8.105 \text{ mm}/\mu\text{s}$ for RDX/graphite (99.5/0.5) and density 1.63 g/cm^3 (Fig 11)

^c Average explosive column thickness from Table 2

Table 22

Lead cup No. 4, time measurements from DEE-profile

Test Assembly: 18.2 in Fig 18, Tests No. 144-162, 18.3 in Fig 18, Tests No. 163-165
 Variables: Barrier hole, standoff L, M55 Detonator

Test No.	Assembly (inches)		Source of M55 ^c	Time (nanoseconds) ^a					Detonation Effect ^d
	Hole dia	Standoff L ^b		t _{shock}	t _{frag}	t _{det}	t _{end}	t _{OT}	
144	.078	.0908	LS	410	620		920	1026	Yes
145								999	Yes
146				310	510	720	880	848	Yes
147				420	600	830		1245	Yes
148				370	510	690	880	883	Yes
149	.078	.0908	KN	450	(e)		1360	1843	No
150	.078	.0648	KN	280		440		922	Yes
151		.0648		(190)	(e)	520	820	796	Yes
152		.0648		260		720	1280	1303	Yes
153	.078	.0648	KN	240			1500	147	Inert
154		.0648		260	(e)			30288	Inert
155	.038	.0908	IOP	no signals				11051	No
156								7123	No
157									No
158	.078	.0908	IOP	420	800		1240	(1437)	No
159				440	600	840	960	1118	Yes
160				340	660	800	980	1158	Yes
161				400	700		1040	1201	Yes
162				400	800		1080	1214	Yes
163	.250	.0883	IOP	460	720	880	1040	1093	Yes
164				280	440	840	960	975	Yes
165				380	680	860	1000	1055	Yes

^a Measured with the accuracy of the time scale units on scope graticule, (see Fig 20 & 21)

^b L = .0648" is caused by .035" instead of .061" thick barrier washer

^c M55 Detonator Lots: LS-DZ-3347, KN-E-26, IOP-1-74

^d Lot KN-E-26, closure with Teflon/paper laminate gives no effective fragmentation

^e In reference to Item 10, Fig 18, "Yes"/"No" means "Was deformed"/"Not deformed"

Table 23

Lead cup No. 4, velocities of shock and fragments^a

Test No.	Assembly (inches)			Velocity (m/sec)		Detonation Effect
	Hole dia	L	M55	v _{shock}	v _{frag}	
144	.078	.0908	LS	5625	3720	Yes
145						Yes
146				7440	4522	Yes
147				5491	3844	Yes
148				6233	4522	Yes
Average				6197±731	4152±354 ^b	
149	.078	.0908	KN	5125	(c)	No
150	.078	.0648	KN	5878	(c)	Yes
151					(c)	Yes
152				6330		Yes
153	.078	.0648	KN	6858		inert
154				6330	(c)	inert
155	.038	.0908	IOP	no signals		No
156				in the lead		No
157						No
158	.078	.0908	OP	5491	2883	No
159				5242	3844	Yes
160				6783	3494	Yes
161				5766	3295	Yes
162				5766	2883	Yes
Average				5810±431	3280±303 ^b	
163	.250	.0883	IOP	4876	3115	Yes
164				8010	5097	Yes
165				5902	3298	Yes

^a Calculated with values of Table 22

^b 90% confidence interval

^c Lot KN-E-26, closure with Teflon/paper laminate

Table 24**Influence of gap on shock and fragment velocities
of M55 detonators^a**

M55 lot	Number tested	Shock (m/s)	Fragments (m/s)
		Gap 1.000 ^b	
LS-DZ-3347	7		3617±165
		Gap 0.091 ^c	
LS-DZ-3347	4	6197±731	4152±354
IOP-1-74	5	5810±431	3280±303
		Gap 0.068 ^d	
IOP-1-74	5	5764±417	3679±143

^a Mean values and their 90% confidence intervals

^b See Table 1 of Ref 13

^c Values from Table 22

^d Values from Table 20 for 5 mil foil on lead explosive

Table 25

Calculated excess transit times for lead cup No. 4 with a 0.091" gap

Test No.	M55 Lot	t_{OT} (ns) ^b	h (in.)	t_{id} (ns) ^c	$t_{cal,fr}$ (ns) ^d	$t_{cal,sh}$ (ns) ^d
126	LS-DZ-	908	0.0997	298	55	238
127	3347	820	0.1019	304	-39	144
128		901	0.0996	297	49	232
129		881	0.1007	301	25	208
130		883	0.1009	301	27	210
131		900	0.1010	302	43	226
144		1026	0.0998	298	173	356
145		999	0.1003	300	144	327
146		848	0.1010	302	-9	174
147		1245	0.1006	301	389	572
148		883	0.1009	301	27	210
158	IOP-	(1437)	0.1009			
159	1-74	1118	0.1001	299	116	422
160		1158	0.1019	304	151	457
161		1201	0.10	299	199	505
162		1214	0.10	299	212	518

^aTests No. 126 to 131 in test assembly 2.1 shown in Fig 2; Tests No. 144 to 148 and No. 158 to 162 in test assembly 18.2 shown in Fig 18; Test No. 158 gave a no-fire for LC No. 4

^bData from Tables 13 and 22

^cIn $t_{id} = h/v_d$, $v_D = 8.504$ mm/ μ s for LC No. 4 explosive RDX/graphite (99.5/0.5) with density 1.74 g/cm³ (Fig 11)

^dIn $t_{cal,fr}$ and $t_{cal,sh}$ are contained t_{frag} and t_{shock} (see Table 14)

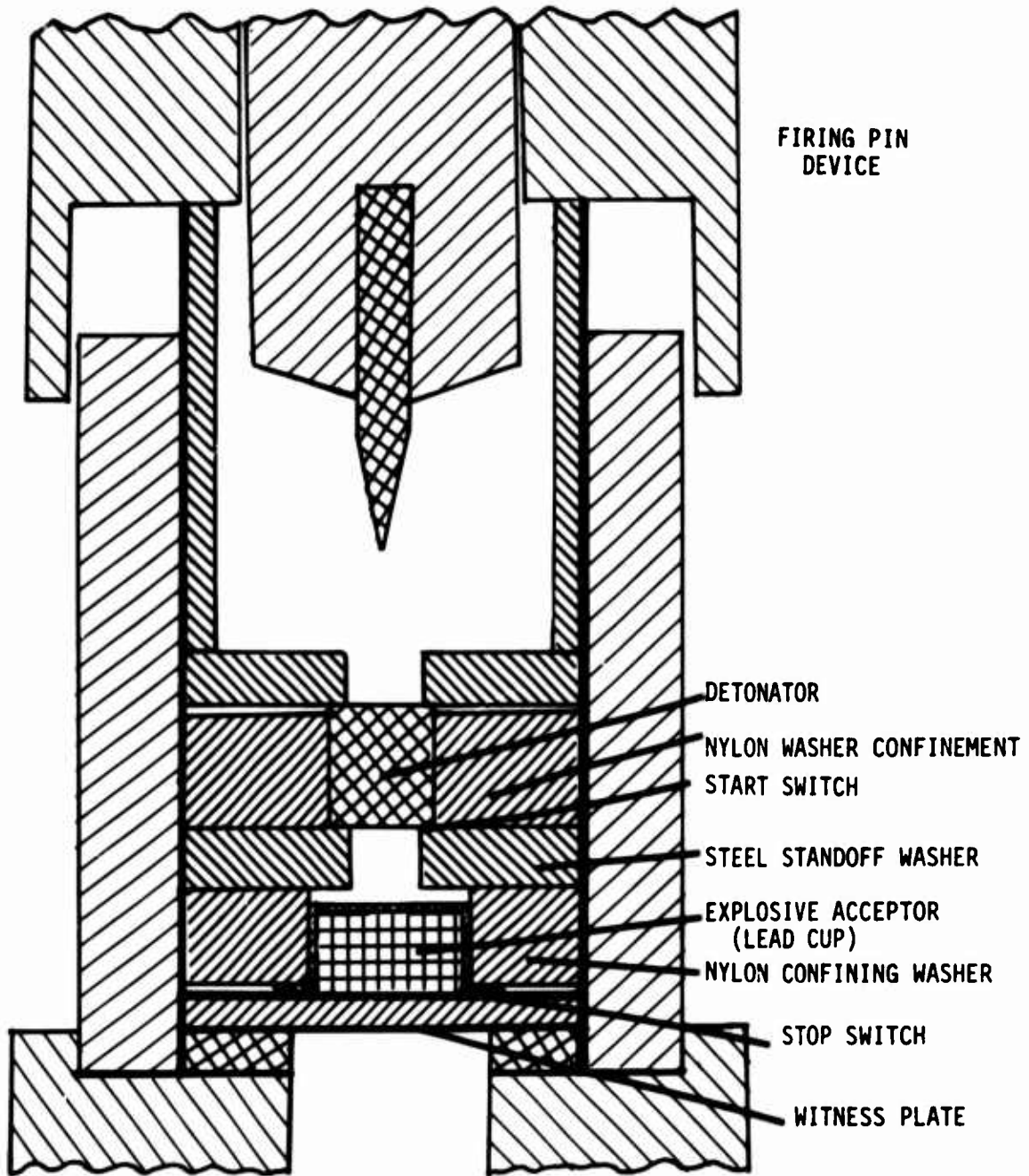
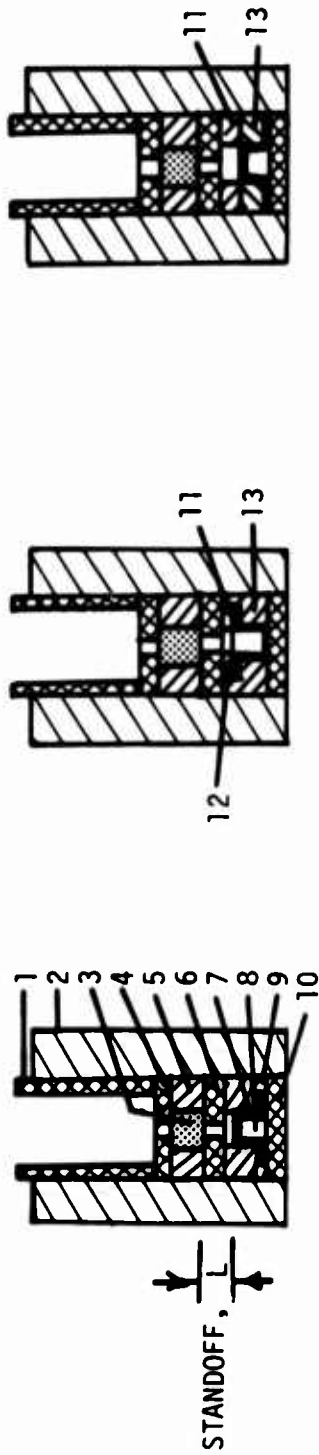
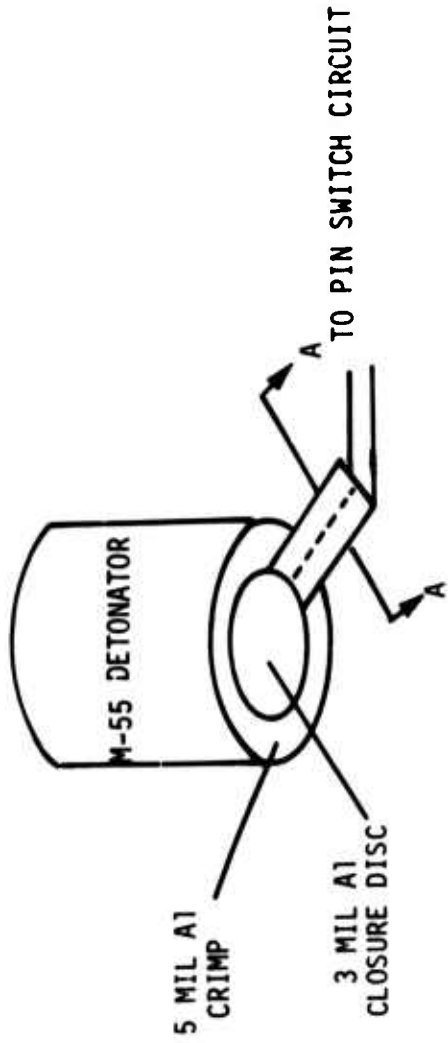


Fig 1 Test apparatus for overall transit time measurements



- | | | | |
|-----------|-------------------|-----|-----------------------|
| 1. | Al Tube | 6. | Steel Standoff Spacer |
| 2. | Lucite Tube | 7. | Al Cup |
| 3. | M-55 Detonator | 8. | Pressed Explosive |
| 4. | Steel Washer | 10. | Witness Disc |
| 5, 9, 13. | Nylon Confinement | 11. | Nylon Standoff Washer |
| | | 12. | Al Foil Cover |

Fig 2 Test assemblies for t_{OT} measurements



VIEW A-A

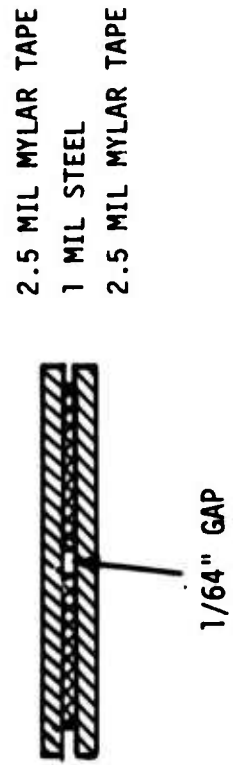
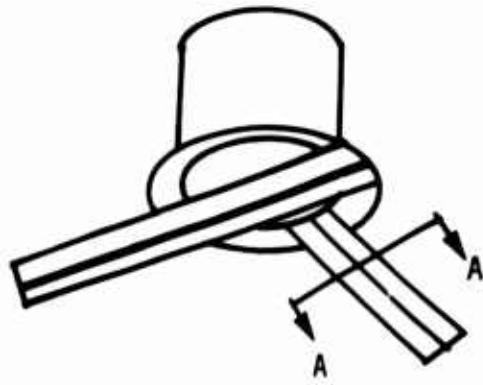


Fig 3 Start trigger switch at base of detonator



POSITION 1

VIEW A-A



SWITCH NO. 1



SWITCH NO. 2

Fig 4 Stop trigger switches

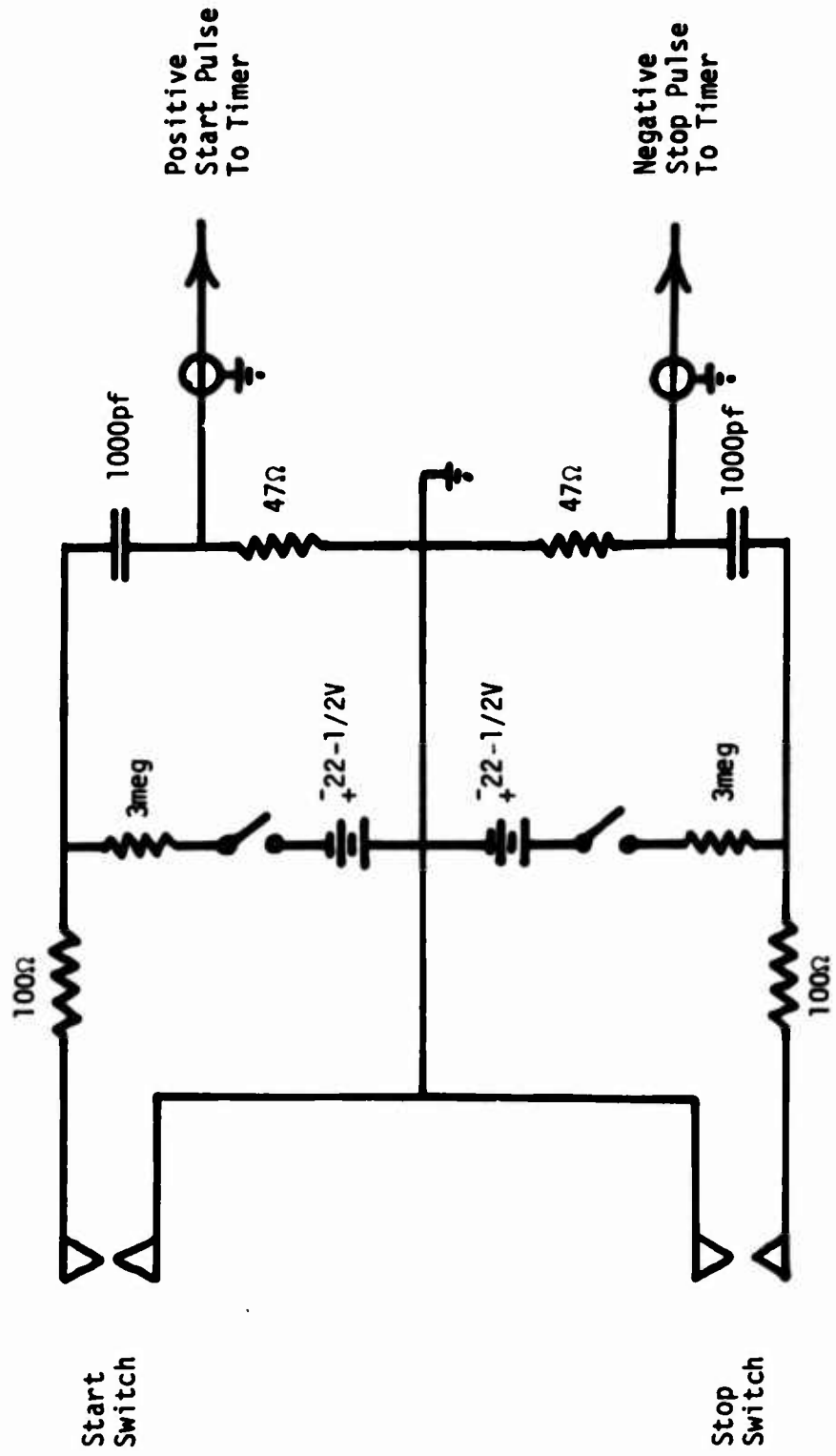


Fig 5 Pin switch circuit

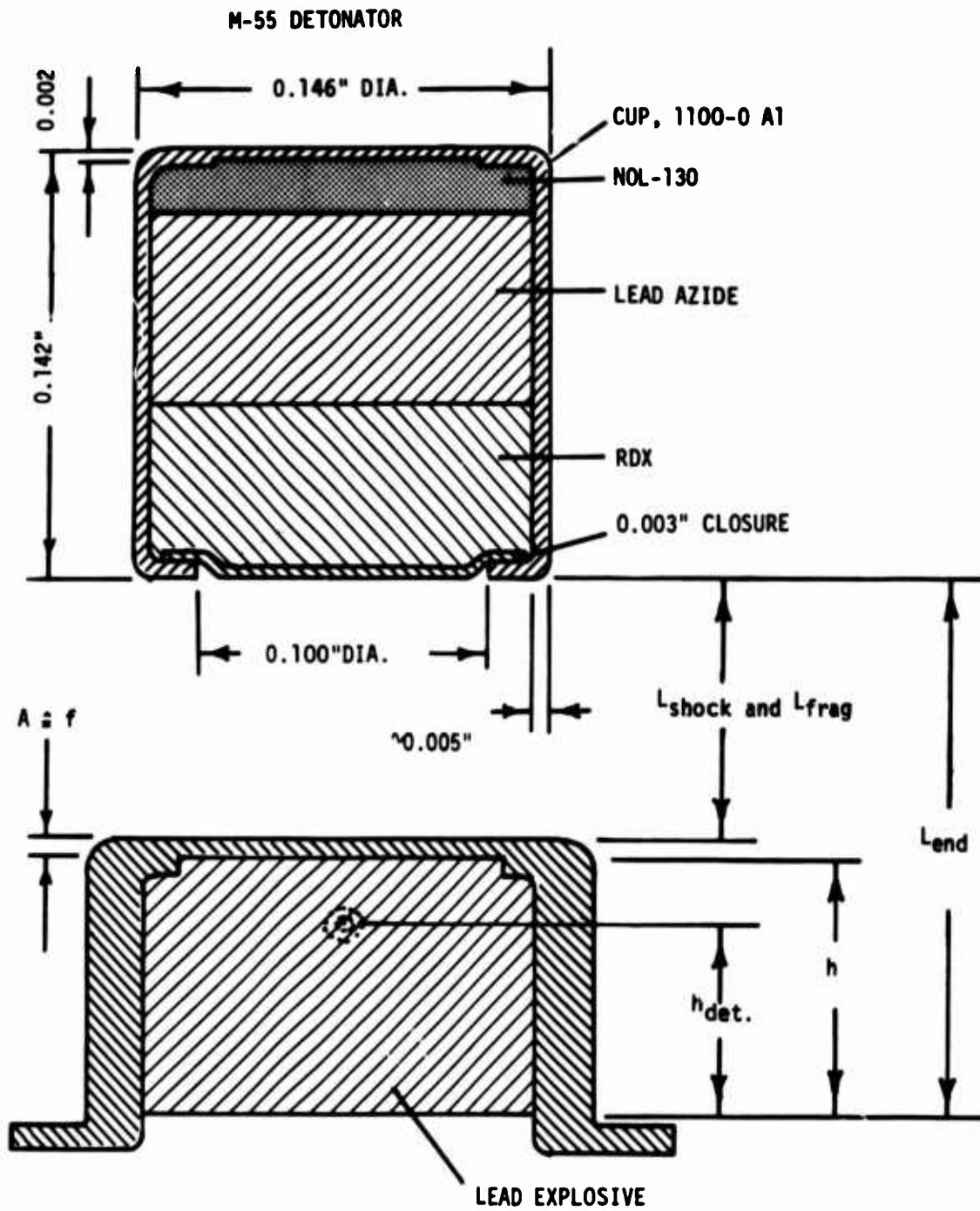


Fig 6 Illustration of detonation effect explosives configuration

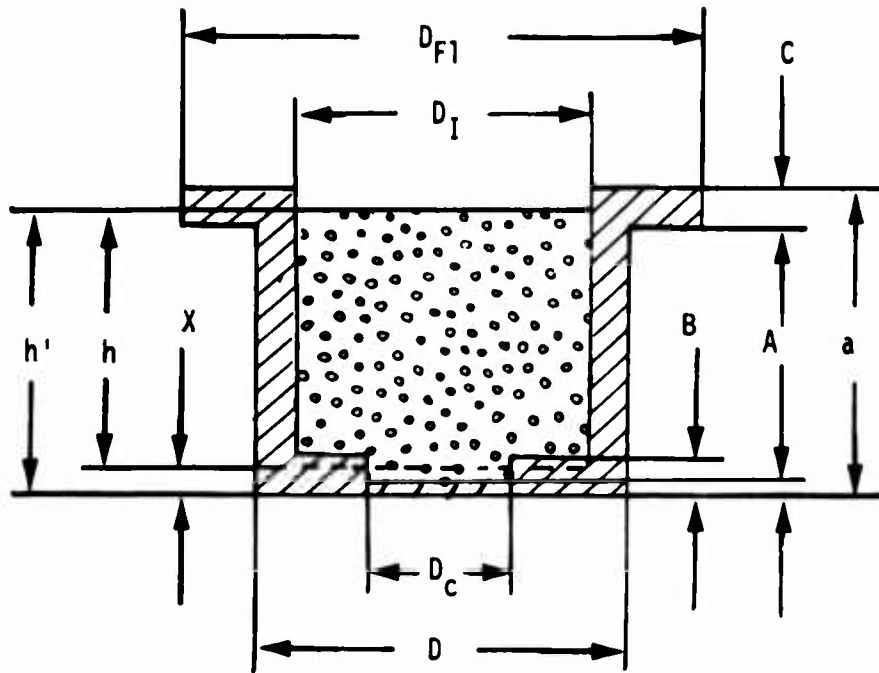


Fig 7 Lead cup dimensions

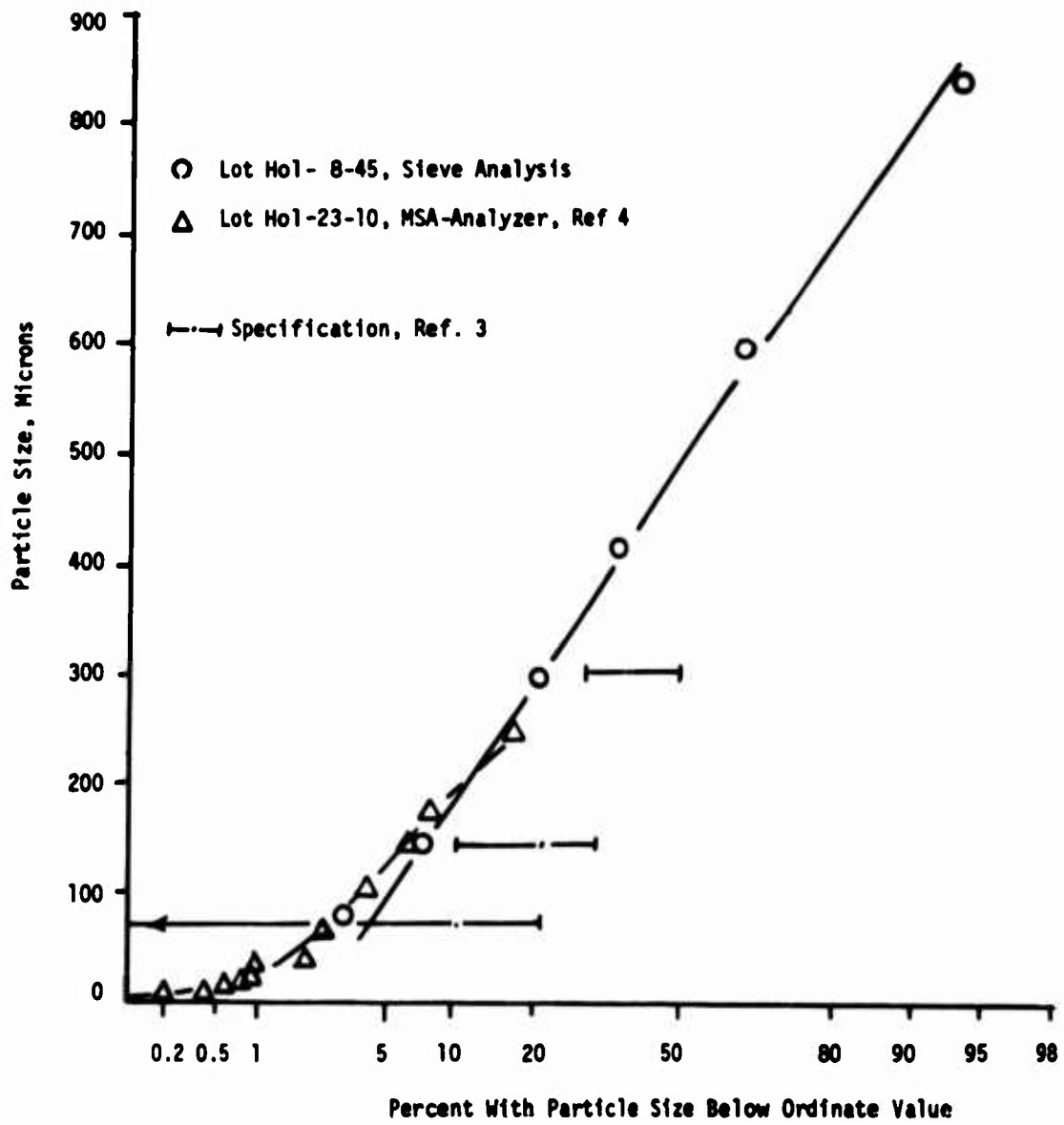


Fig 8.1 Particle size distribution of RDX, Class C

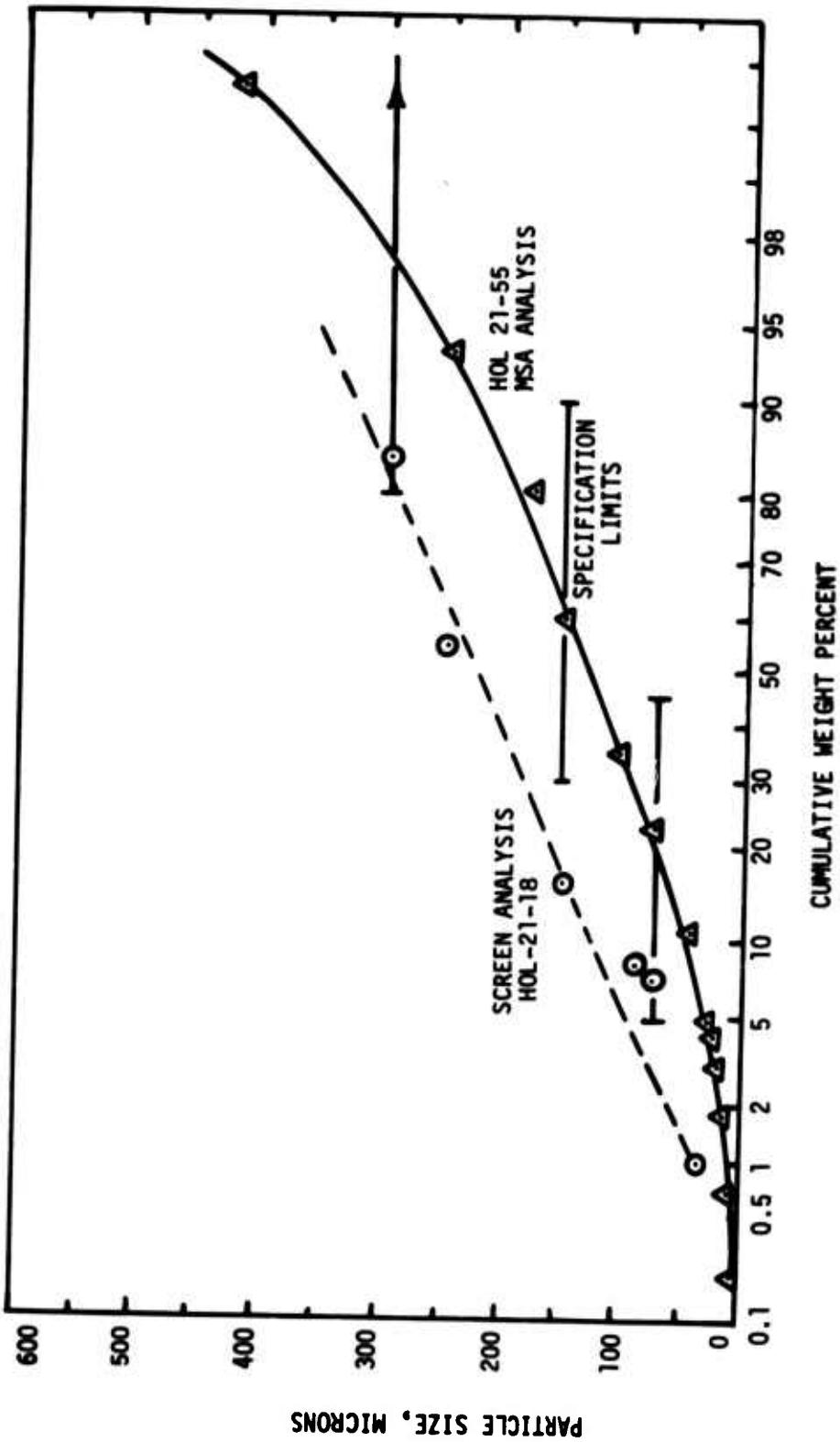


Fig 8.2 Particle size distribution of Class A RDX

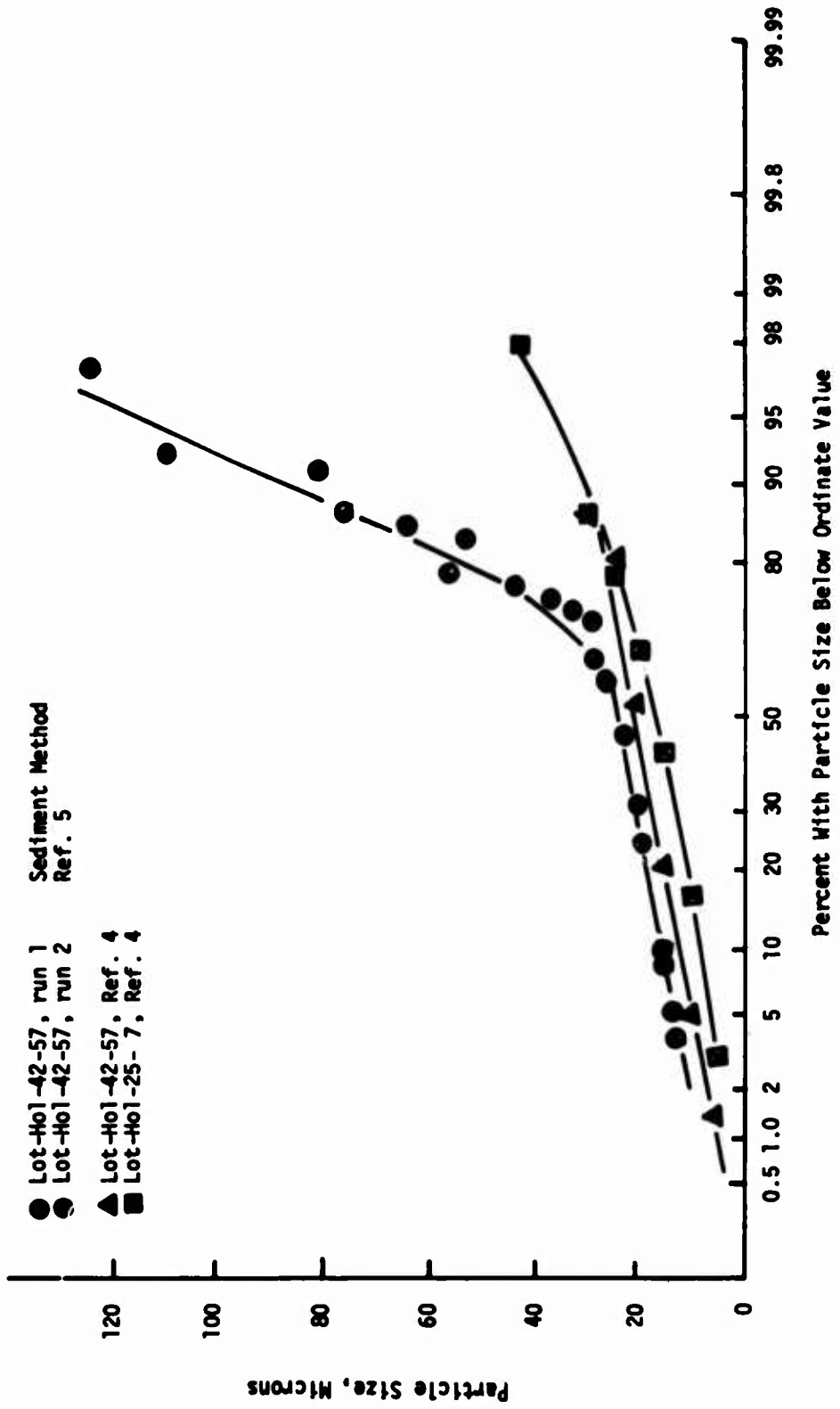


Fig 8.3 Particle size distribution of RDX, Class E

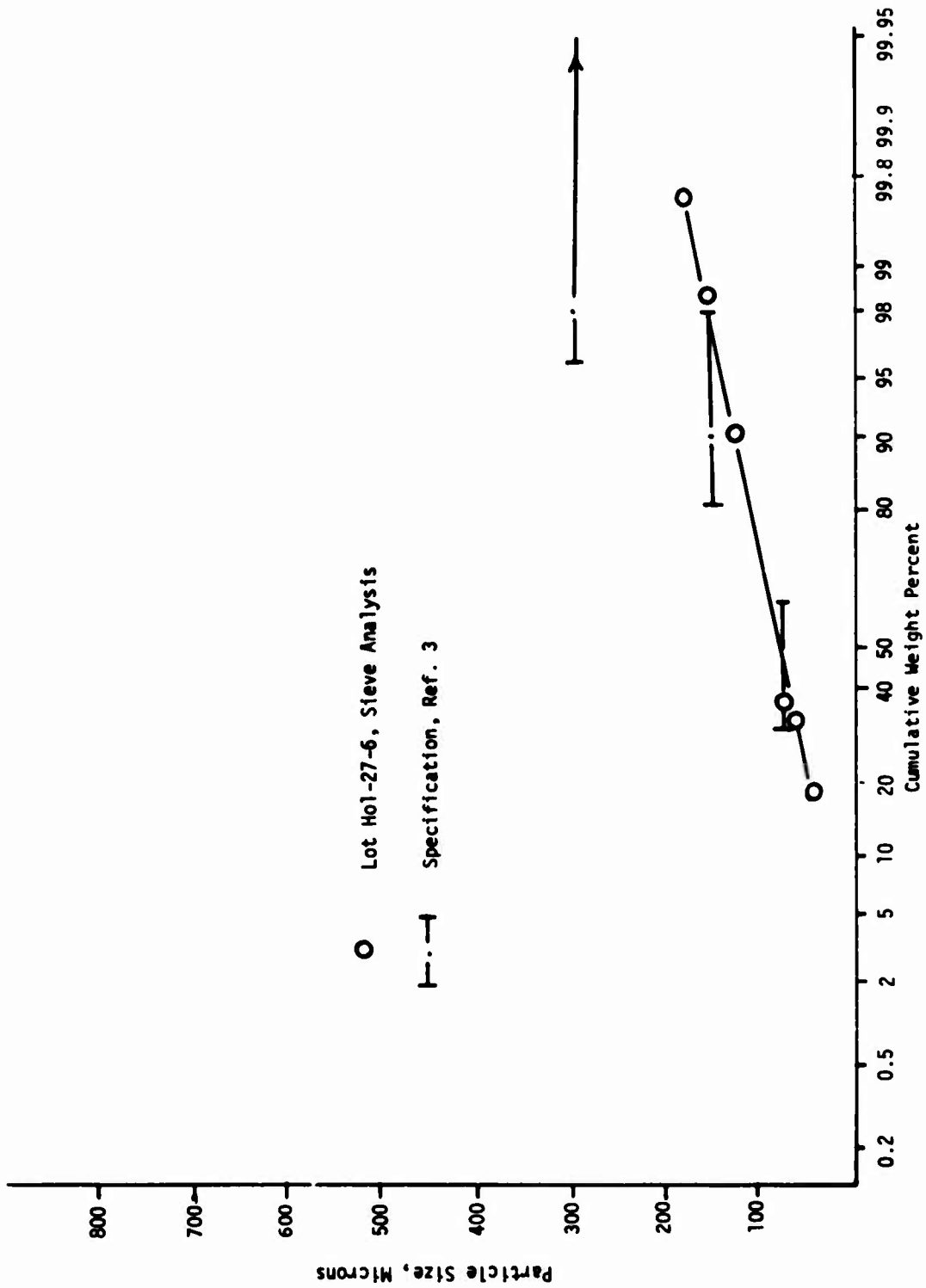


Fig 8.4 Particle size distribution of RDX, Class C

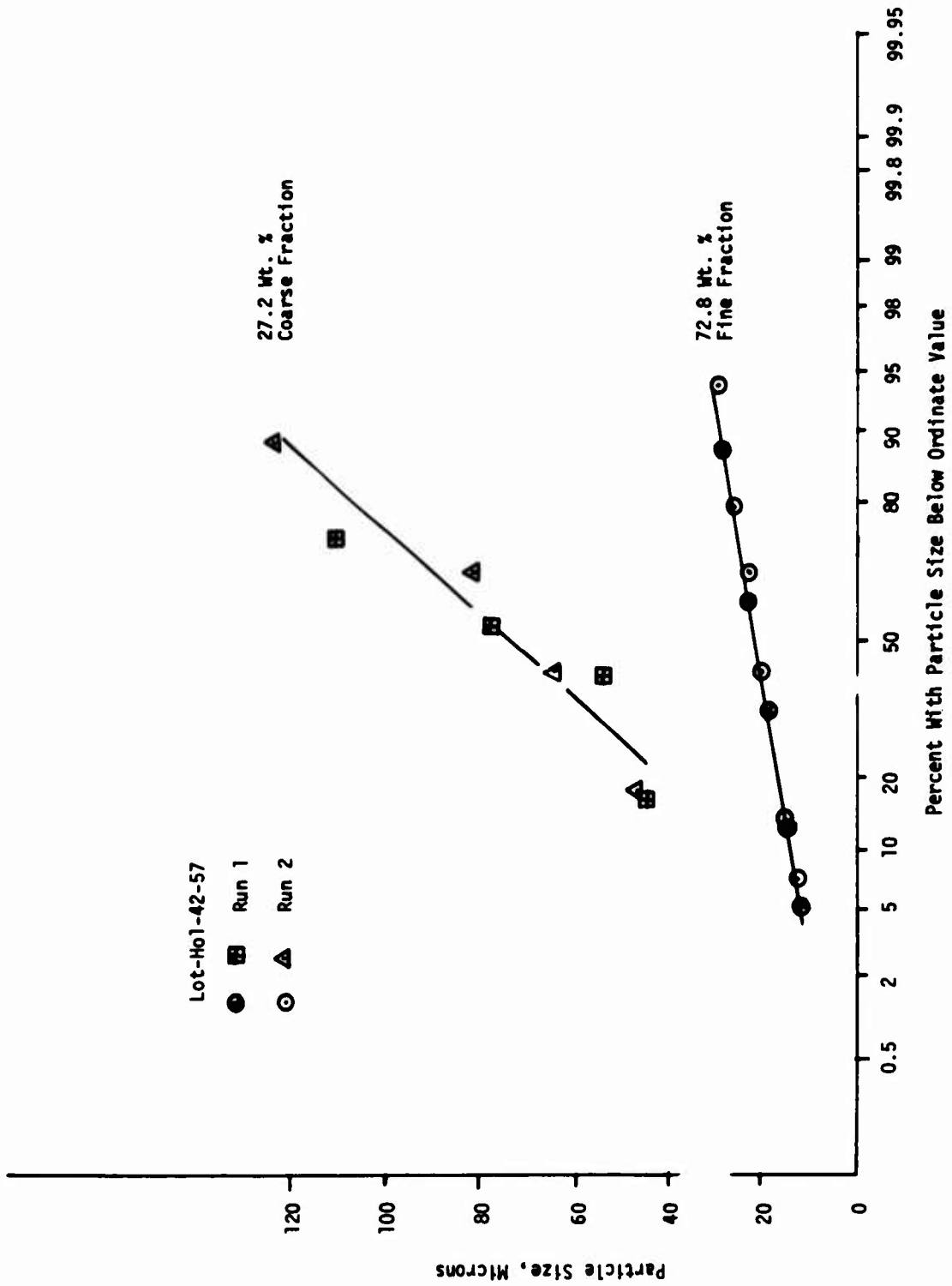


Fig 8.3.1 RDX Class E, fractions 22 μ and 74 μ

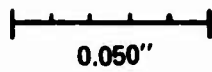


Fig 9 Lead cup No. 4 - photograph of a cut through the aluminum case parallel to the center axis (height = 0.1104 in.)

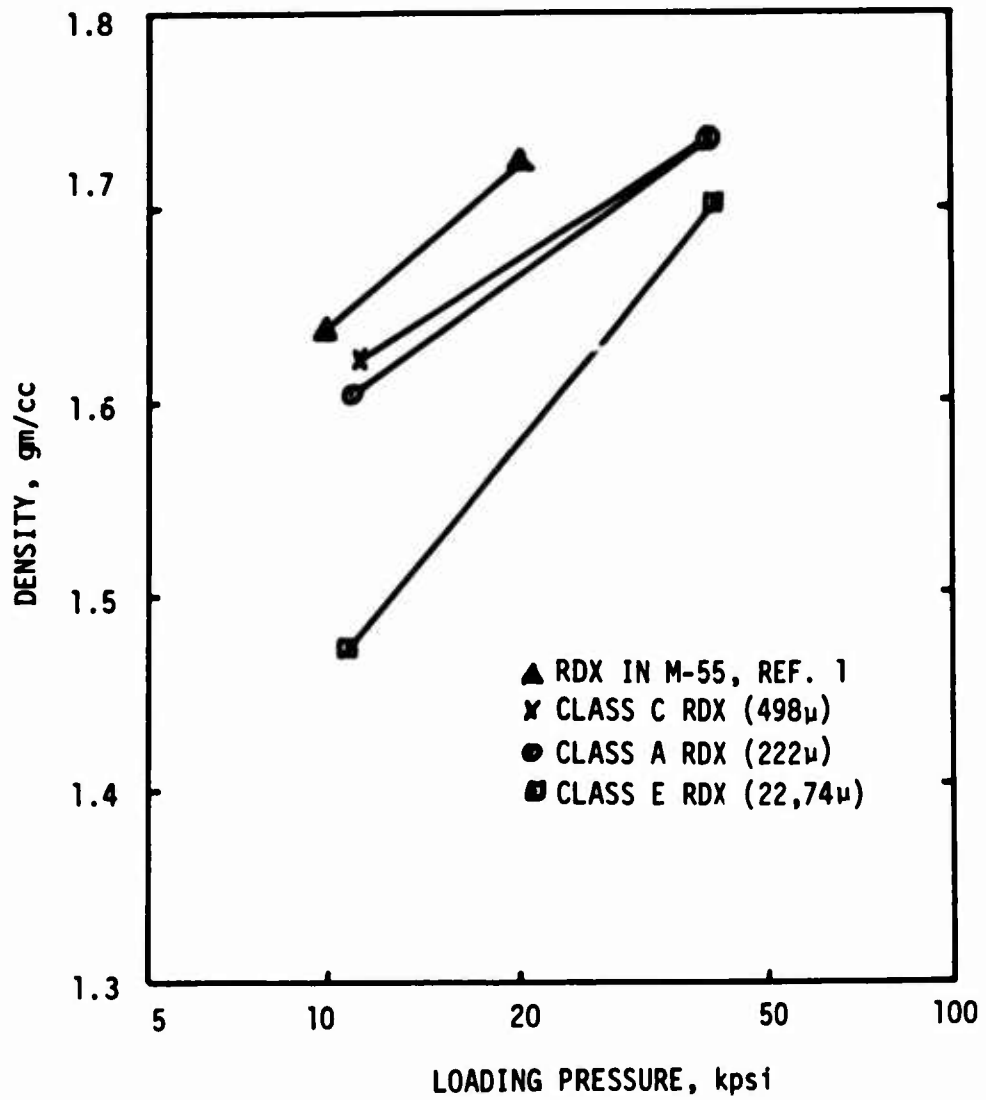


Fig 10 Influence of RDX particle size and loading pressure on the compacted density

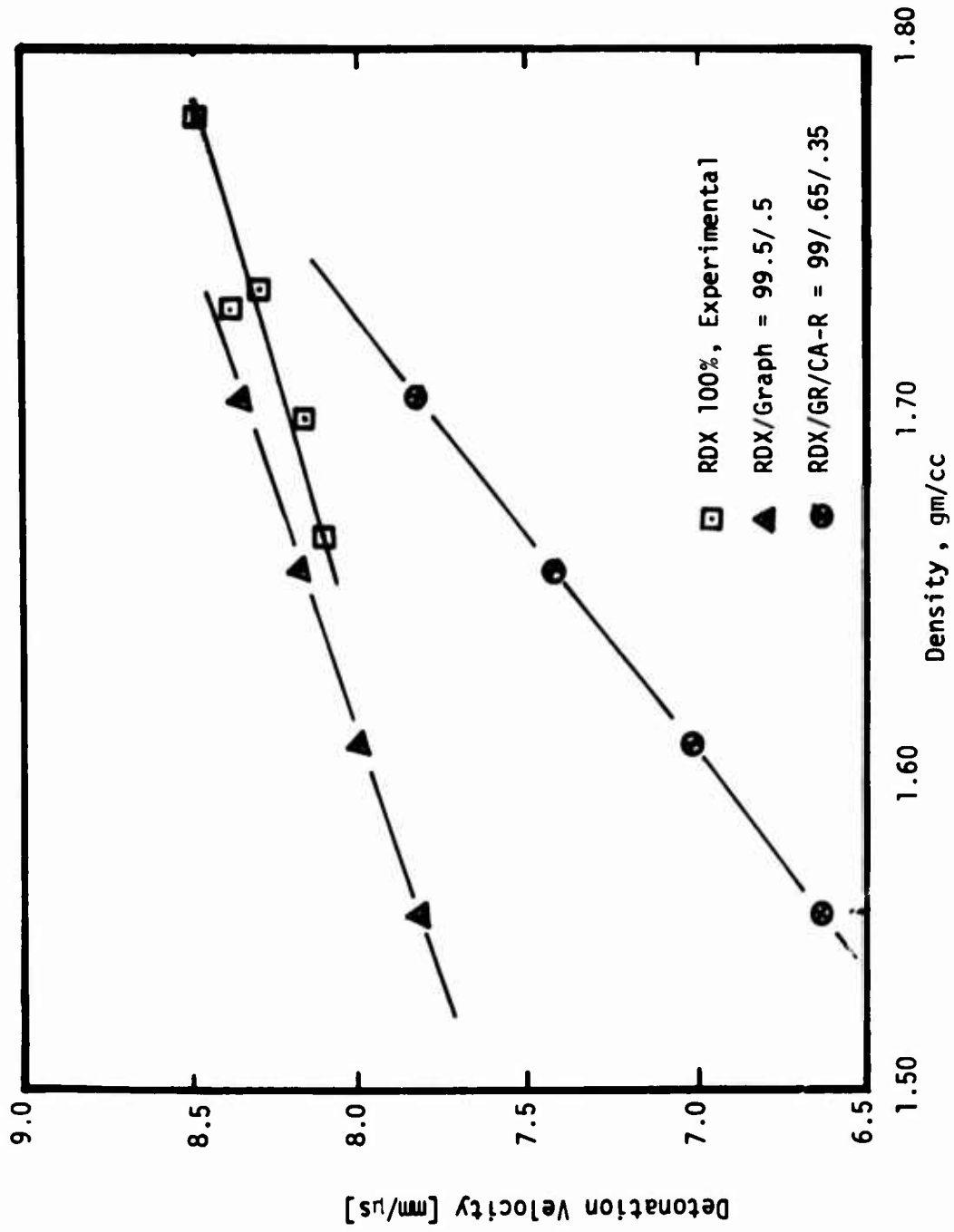


Fig 11 Detonation velocity vs density of RDX

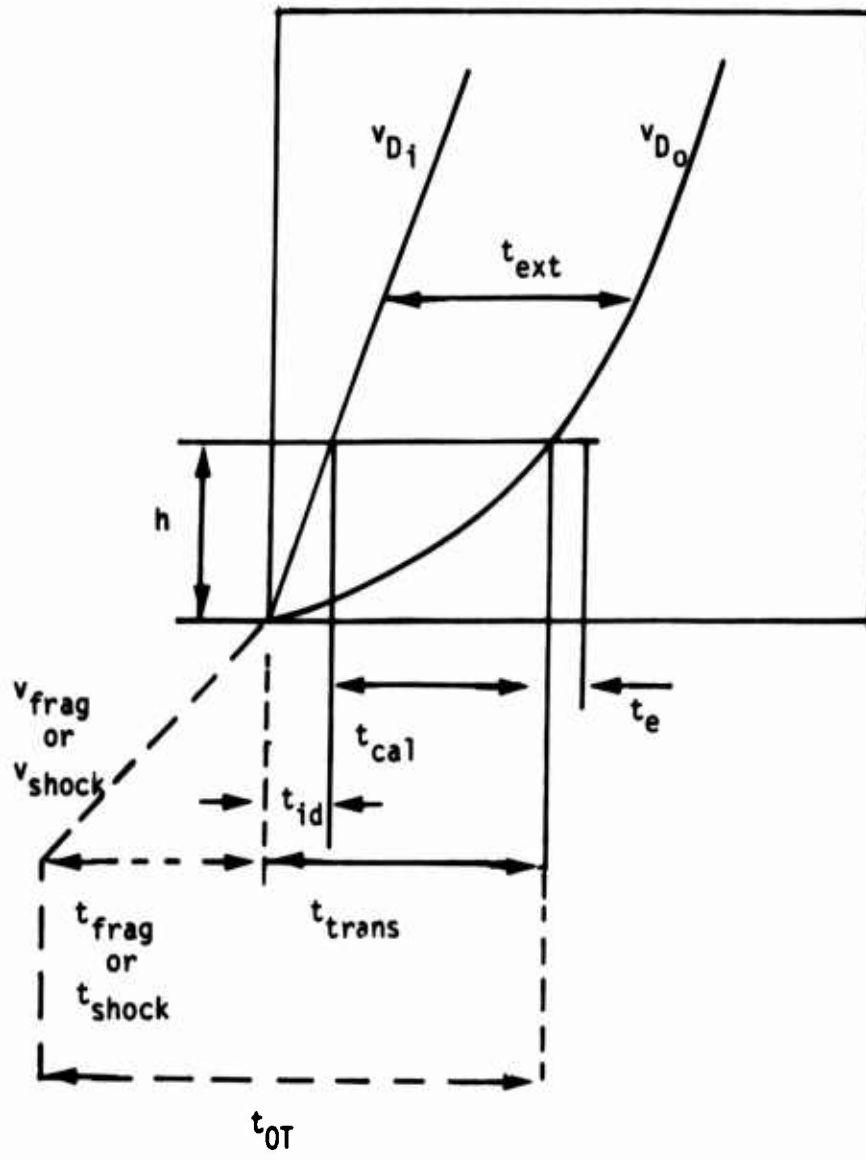


Fig 12 Space-time plot of shock initiation (Ref 8)

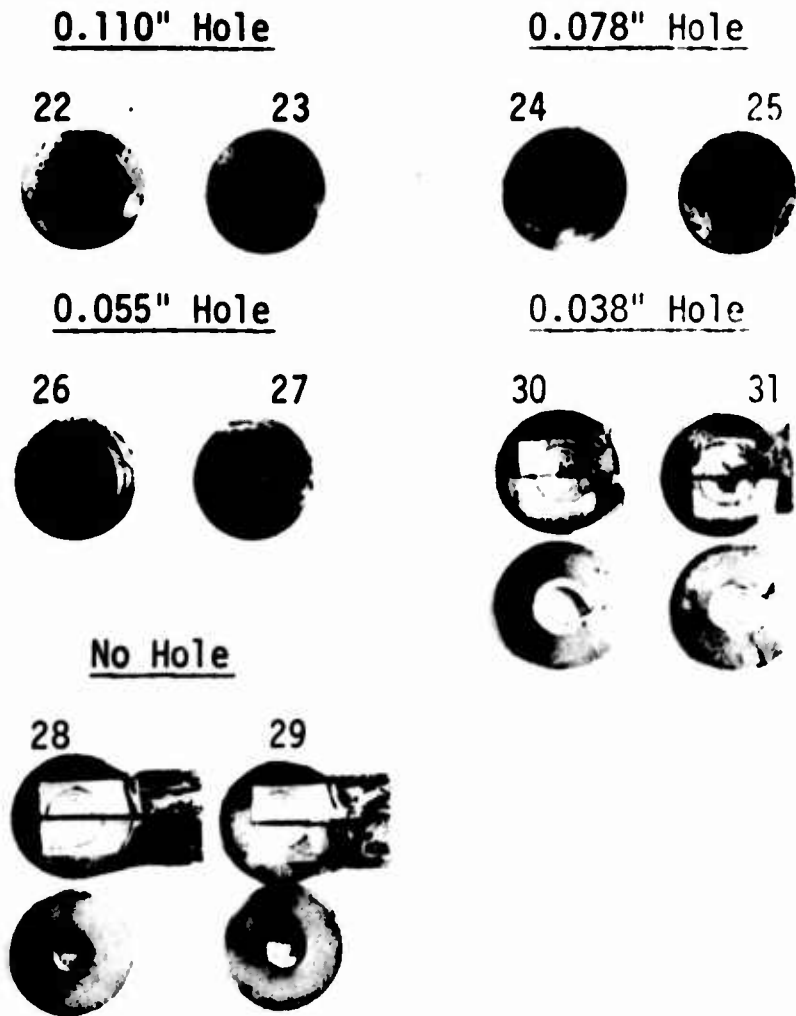
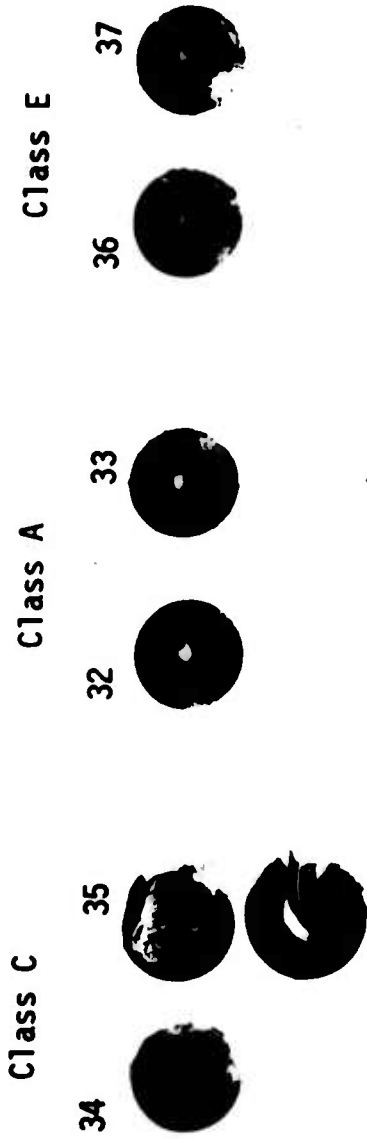


Fig 13 Witness disc penetration in relation to the hole diameter in the standoff spacer (Configuration 2.1 of Figure 2 with 0.0864" spacing)

11000 PSI



40000 PSI

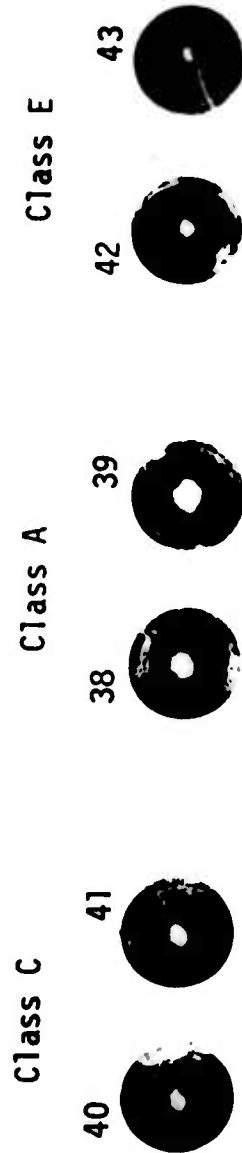
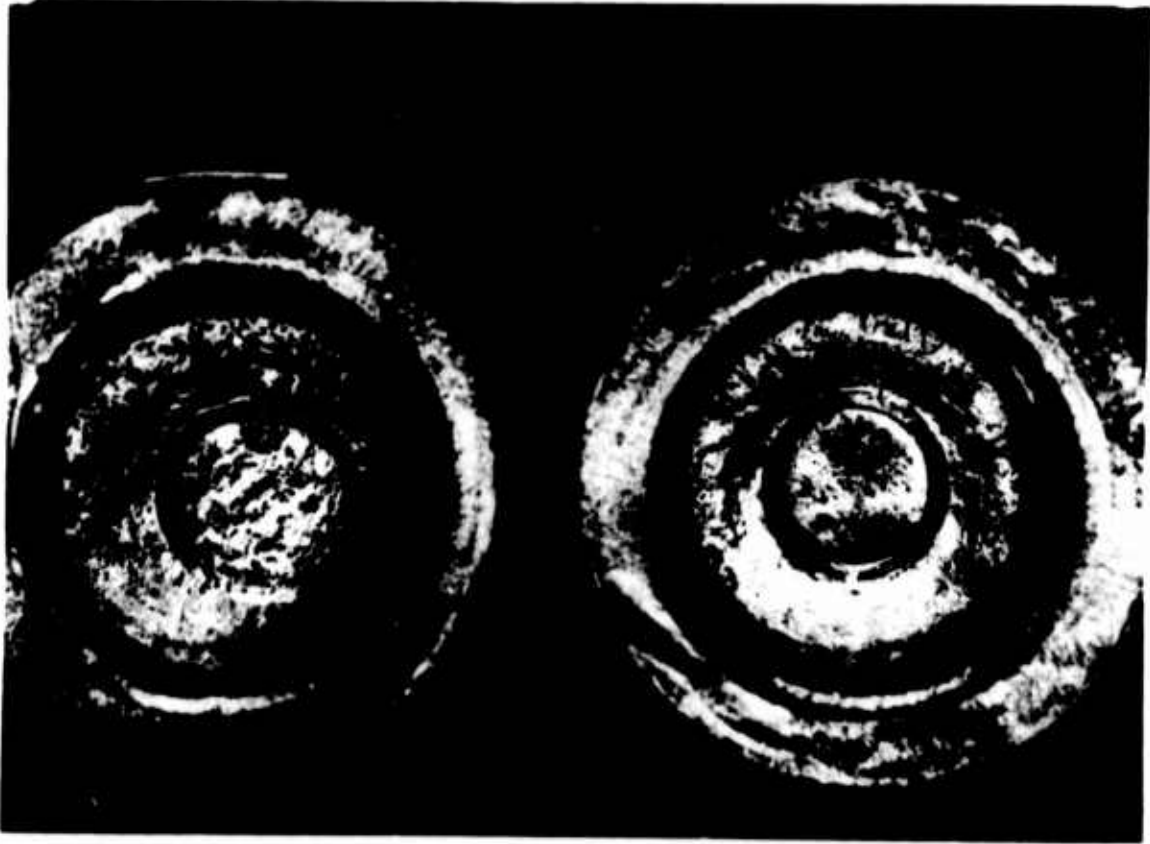


Fig 14 Witness disc penetration (by lead cup No. 1) in relation to RDX particle size (Class C, A, E) and loading pressure



15.1

15.2

15.1: coin off center .077 diameter (See Table 1)
15.2: coin in center

**Fig 15 Lead cup No. 3: Photograph of the coined bottom
(see Figure 4), scale ca. 14:1**

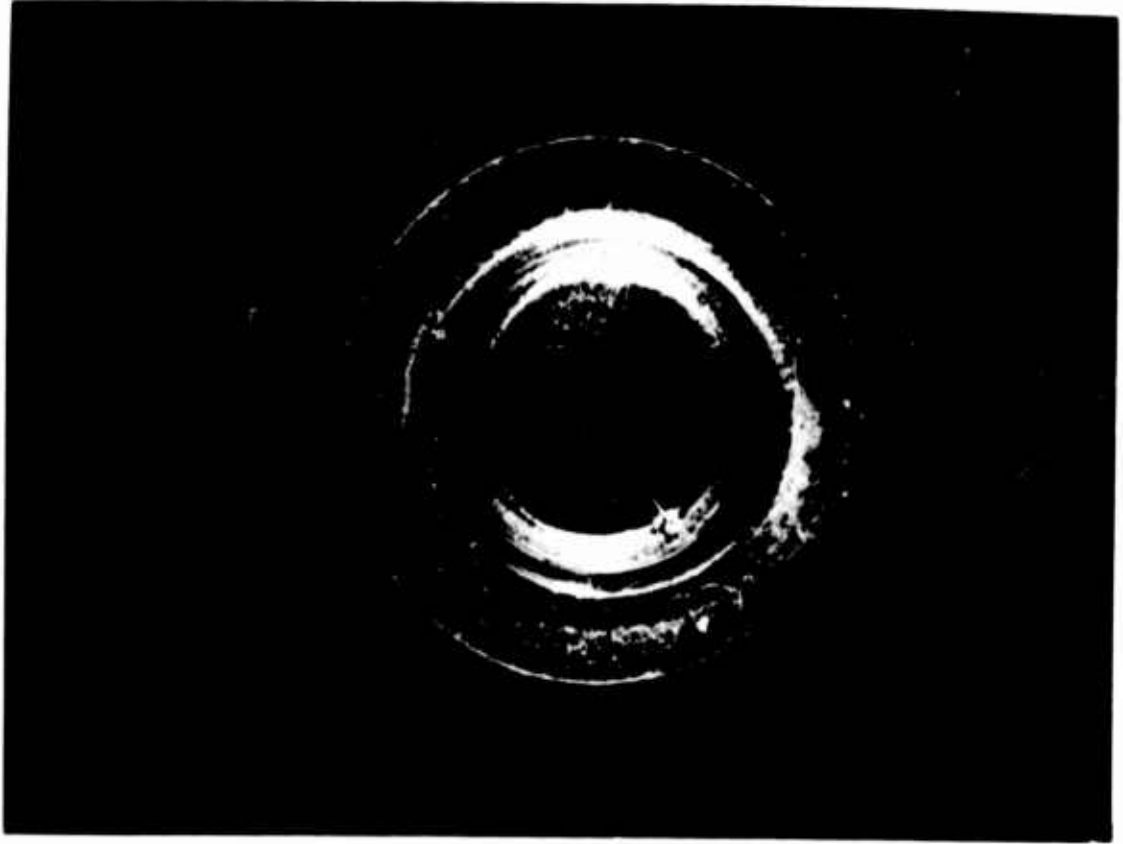


**Fig 16 Lead cup No. 4: Photograph of the bottom area
(see Figure 4), scale ca. 13.5: 1**

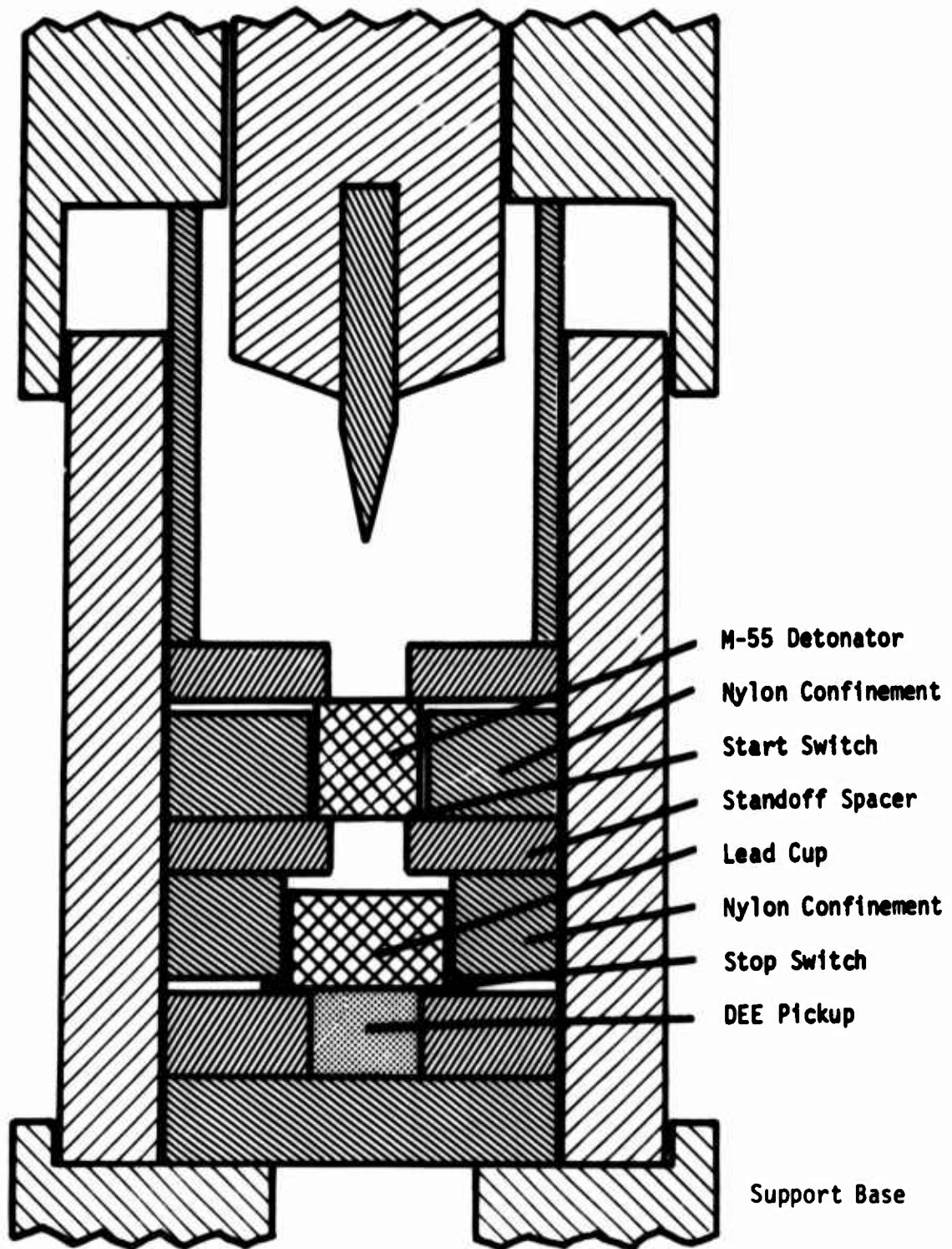
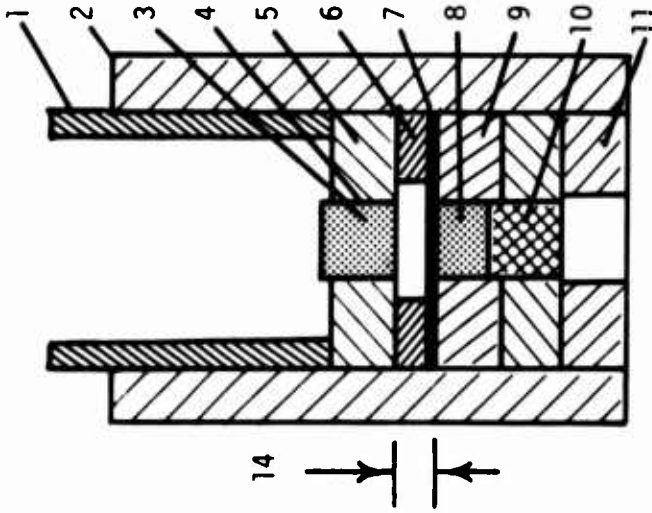
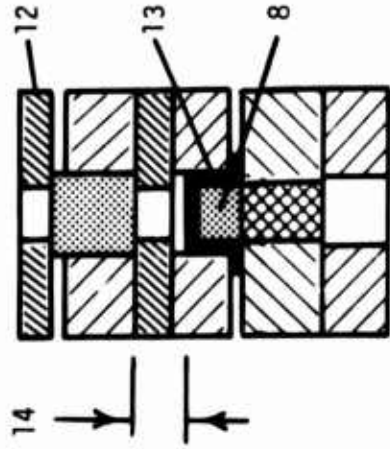


Fig 17 Detonation transfer and detonation electric assembly



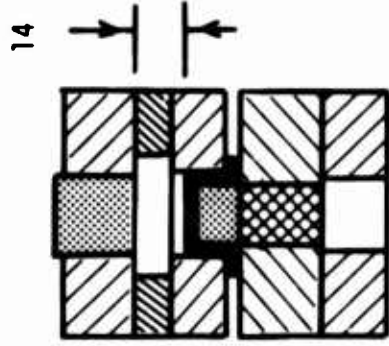
18.1

- 1. Al Tube
- 2. Lucite Tube
- 3. M-55 Detonator
- 4. Glue



18.2

- 5,9. Nylon Confinement
- 6. Standoff Spacer
- 7. Al Foil
- 8. Pressed Explosive
- 10. Pickup Probe
- 11. Nylon



18.3

- 12. Steel Washer
- 13. Al Cup
- 14. Detonator to Acceptor Gap (L)

Fig 18 Test assemblies for DEE and overall transit time measurements

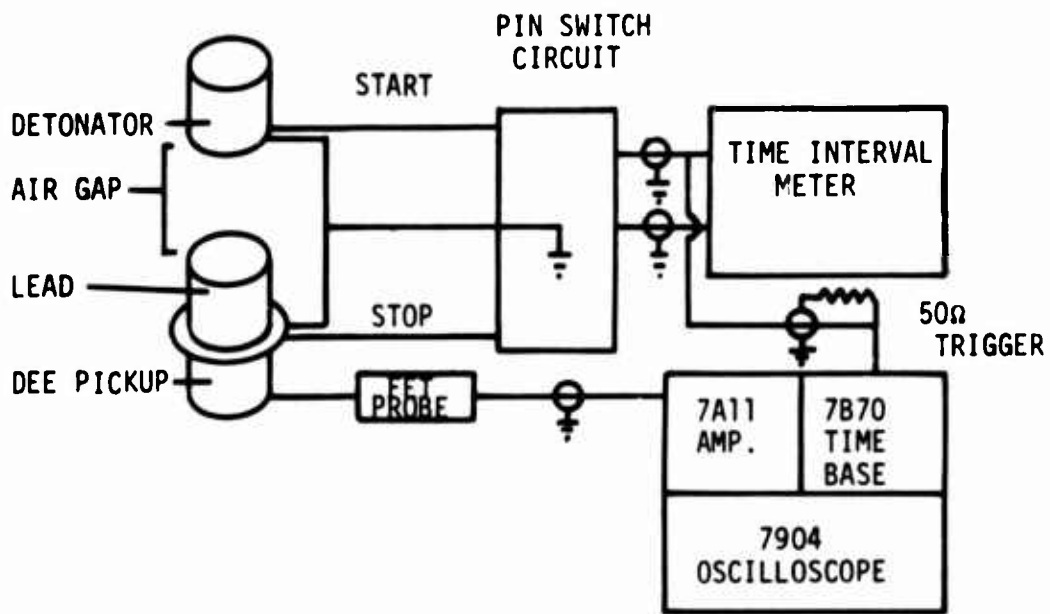


Fig 19 Circuit diagram for transit time (t_{OT}) and DEE

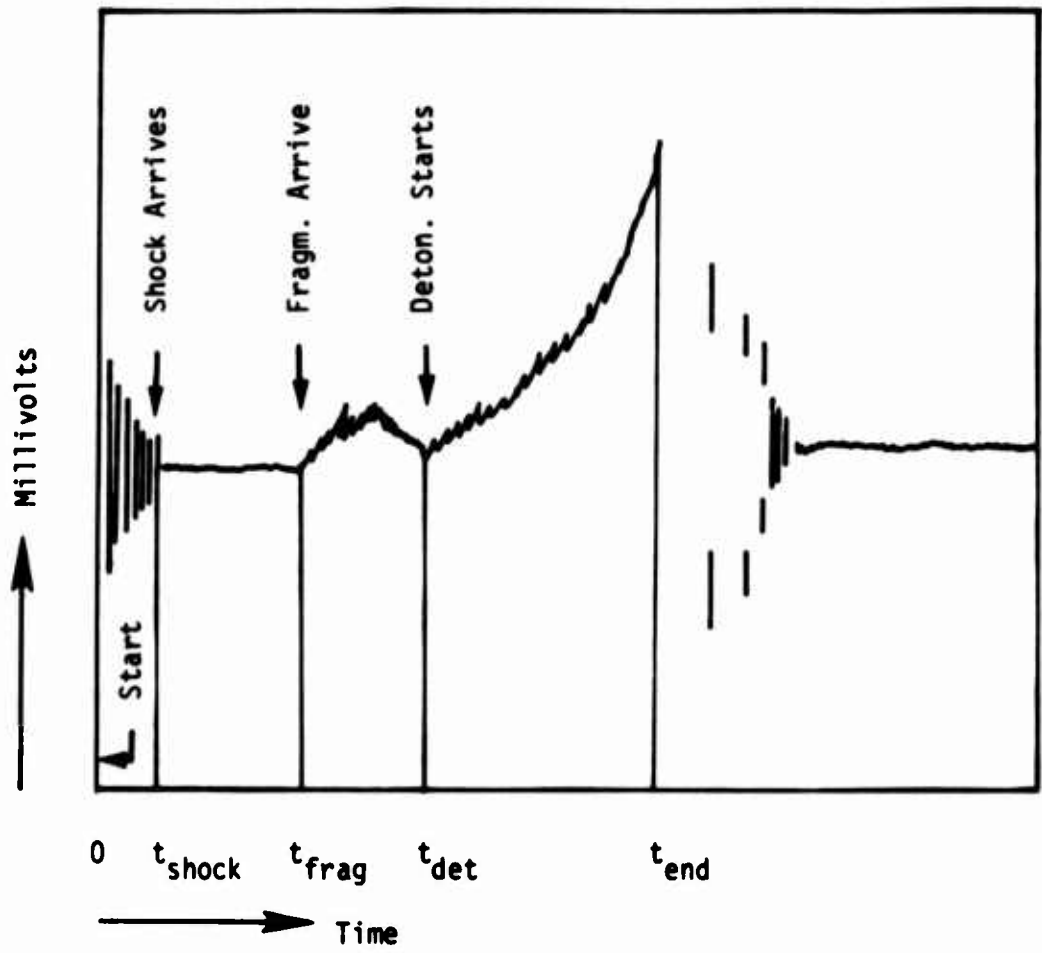
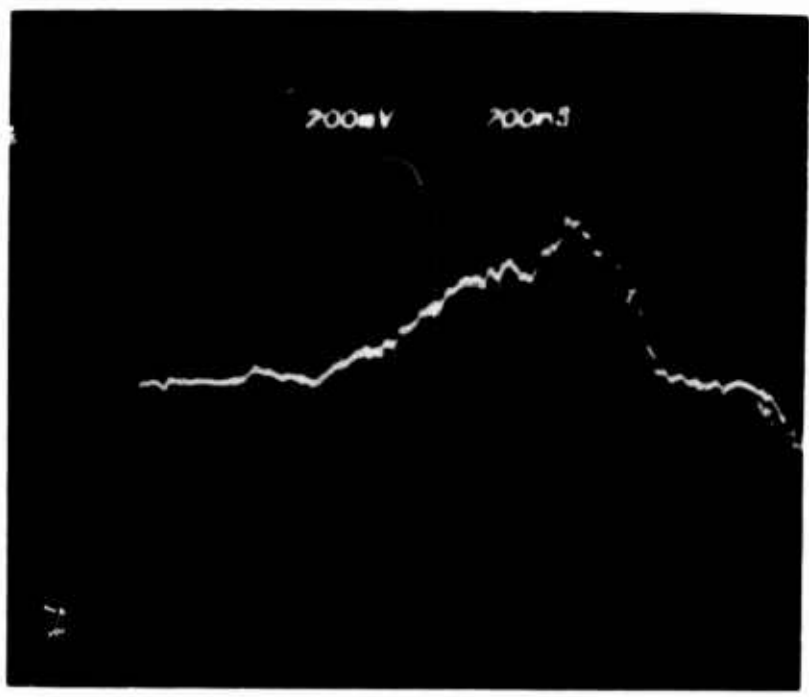


Fig 20 Explanation of the detonation electric effect records



21.1: Test No. 179, Lead Explosive No. 5 from Table 3



21.2: Test No. 189, Pentek as Inert Lead-Filling
(Test Assembly is shown in Figure 18.1)

Fig 21 Detonation electric effect records

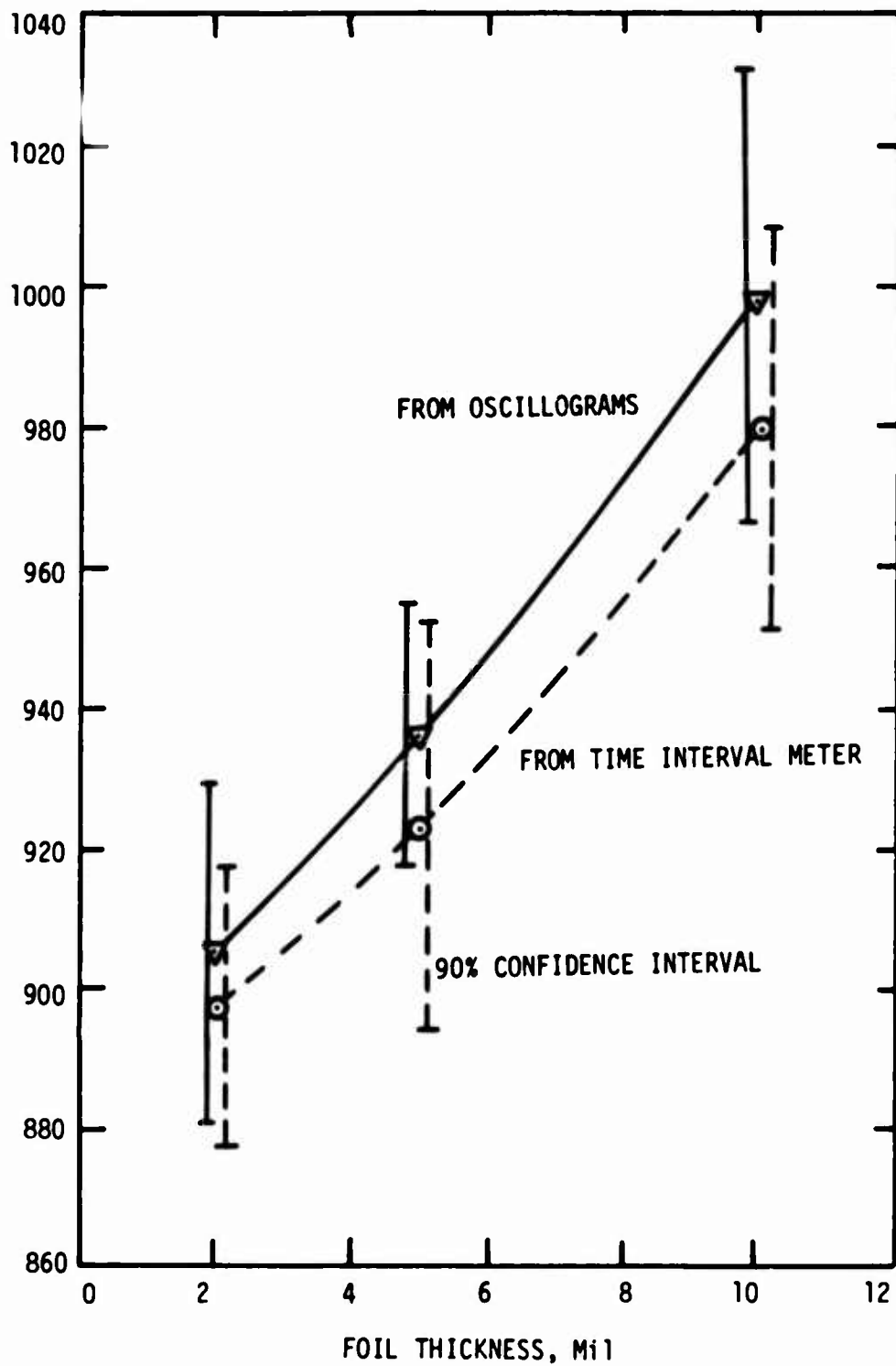


Fig 22 Overall transit time vs foil thickness

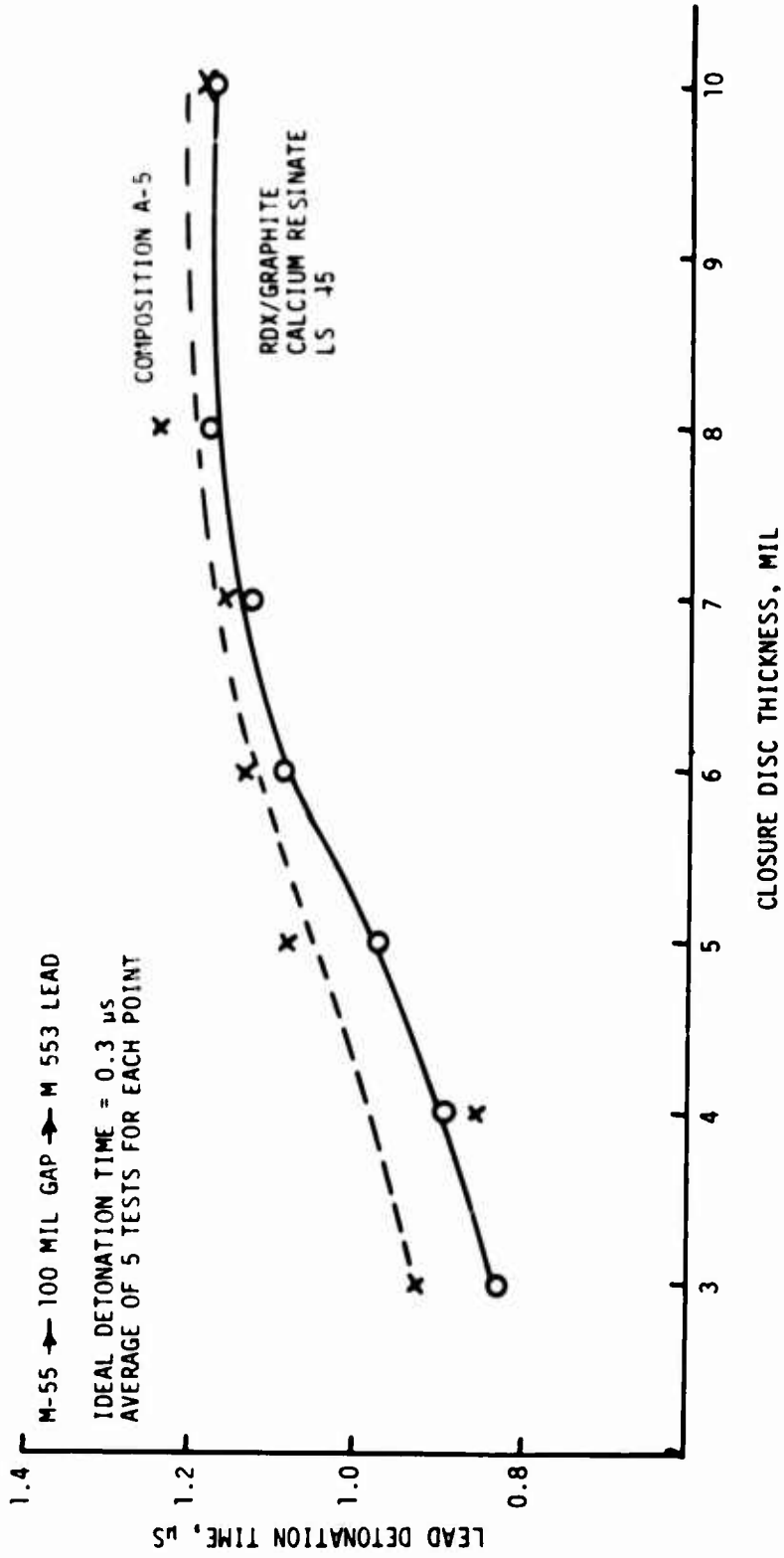


Fig 23 Effect of closure disc thickness on acceptor transit time

APPENDIX

**Effect of Varying M55 Closure Disc Thickness
on Acceptor (Lead) Transit Time**

The transit time measurements in Figure 23 on M553 lead cups were made to determine the effects of variations in M55 detonators and in lead explosives. Transit times in lead cups were measured when initiated by the detonators across a 100-mil gap. Leads and detonators were confined in nylon washers, with a steel washer providing the standoff as shown in Figure 1. The lead cups were the same dimensions as the M219 (Lead Cup #2, Table 2). The M553 leads (LS 745) were loaded with RDX/graphite/calcium resinate by Lone Star AAP and are the same as the M219 leads, while the other special cups were specially loaded by Picatinny Arsenal at 11,000 psi into the same cups.

The detonator variations investigated included thicker aluminum closure discs, use of Teflon-coated paper closure discs, replacement of RDX by HMX, and $\pm 15\%$ variations in RDX content, with compensating variations in NOL-130 content for the high RDX, and in lead azide for the low RDX content as shown in Table A1.

All lead cup explosives were pressed at 11,000 psi. Variations investigated included: Standard Comp A-5 made with Class C RDX; a special Comp A-5 made with Class E (fine particle size) RDX; 99% Class C RDX, 0.65% flake graphite, 0.35% calcium resinate; and pure Class A RDX.

None of the variations resulted in significant improvements over the standard M55 in detonation transfer across a 100-mil gap as measured by lead transit times. Although higher RDX content improved performance in some cases, it also increased the variability in performance due to the marginal quantity of lead azide present. As discussed previously, blast is an important factor in initiation of acceptors across short gaps. Since maximum kinetic energy in the fragments is achieved with 6-mil discs, the effect of thicker closure discs in attenuating blast is apparently of more importance than the increased energy in the thicker discs when spacing is 100 mils or less.

Table A1

Modifications evaluated by transit time measurements

Lot	<u>M55 detonator modifications</u>	Fragment Velocity mm/μs	Response of M553 leads, average transit time (microseconds)	
			Standard M553 Lot LS 745 ^a	Loaded with Comp A-5 ^b at 11,000 psi at Picatinny
LS 3672	Standard 3 mil closure	3.756	0.88	0.91
LS 3664	Thicker closure disc, 4 mil	3.668	0.89	0.86
LS 3665	Thicker closure disc, 5 mil	3.478	0.87	1.08
LS 3666	Thicker closure disc, 6 mil	3.328	1.09	1.13
LS 3667	Thicker closure disc, 7 mil	3.233	1.12	1.16
LS 3668	Thicker closure disc, 8 mil	3.042	1.18	1.14
LS 3669	Thicker closure disc, 10 mil	2.690	1.08	1.18
LS 3670	25 mg in lieu of 19 mg RDX and 12 mg NOL 130 in lieu of 14 mg	3.987	0.95	0.93
LS 3671	15 mg RDX in lieu of 19 mg	3.337	Low Order	Low Order
LS 3673	HMX replacing RDX	3.734	0.96	
KN-E-26	Teflon/paper replacing aluminum closure disc		Low Order	
M553 lead modifications				
LS 3672	Standard M55 detonators	3.756	M553 lead modifications	
LS 3347		3.755	Changed RDX particle size to Class E in Comp A-5 0.87	
			Pure RDX at 1.52 gm/cc, particle size fraction over 74 microns from Class A RDX 0.91	

^a 99% RDX/0.65% calcium resinate/0.35% graphite

^b 99% RDX/1% stearic acid